



Contents lists available at ScienceDirect

Tectonophysics

journal homepage: www.elsevier.com/locate/tecto

Active transpression in the northern Calabria Apennines, southern Italy

L. Ferranti ^{a,*}, E. Santoro ^b, M.E. Mazzella ^a, C. Monaco ^b, D. Morelli ^c^a Dipartimento di Scienze della Terra, Università di Napoli, Italy^b Dipartimento di Scienze Geologiche, Università di Catania, Italy^c Dipartimento di Scienze Geologiche, Ambientali e Marine, Università di Trieste, Italy

ARTICLE INFO

Article history:

Received 11 January 2008

Received in revised form 24 October 2008

Accepted 11 November 2008

Available online xxxx

Keywords:

Morphotectonic analysis

Active thick-skinned transpression

Calabria Apennines

Southern Italy

ABSTRACT

An integrated analysis of geomorphologic and structural data, offshore seismic profiles and local network seismicity, is used to shed light on the hitherto poorly known active deformation field that affects the Southern Apennines orogen in northern Calabria region. In the Southern Apennines, Middle Pleistocene waning of Miocene–Early Pleistocene thin-skinned frontal thrust belt motion toward the Apulian foreland to the NE was coeval to onset of regional uplift, which is documented by flights of raised marine terraces. Short-wavelength (~5–10 km) and amplitude (~20–50 m) undulations are superposed to the regional uplift (~100 km length and ~500 m amplitude scale) profile of Middle–Upper Pleistocene marine terraces on the Ionian Sea coast of northern Calabria stretching along the borders of the Sila and Pollino mountain ranges and across the intervening Sibari coastal plain. The secondary undulations spatially coincide with the last generation of ~W- to ~WNW-striking folds traced in bedrock and locally within Early to Middle Pleistocene continental to transitional deposits. The very recent activity of these structures is highlighted by a range of fluvial geomorphic anomalies and by involvement in folding and locally transpressional faulting of the Middle Pleistocene and younger depositional sequences submerged beneath the continental shelf. We argue that the local-scale, but pervasive undulations in the deformation profile of marine terraces represent shallow-crustal folds grown within a recent and still active transpressional field. A major structural culmination bound by fore- and retro-verging transpressional shear zones is represented by the Pollino mountain range and its offshore extension in the Amendolara ridge, and a further SW-directed transpressional belt is found in northern Sila and adjacent sea bottom. Epicenter distribution and focal solutions of low- to moderate crustal earthquakes illuminate the two NW–SE trending structural belts beneath the Amendolara ridge and northern Sila, where partitioning between thrust and left strike-slip motion occurs in response to ~E to ~NE directed shortening. A local ~NW–SE extension is recorded by fault-kinematic analysis on NE–SW striking fault segments parallel to the coast on the eastern flank of Pollino. These small-length normal faults do not form a through-going lineament, rather they accommodate the seaward collapse of the uppermost crust above the deeper shortening compartment. Conversely, the active transpression testified by geomorphic, structural and seismicity data is accommodated along deep-seated oblique back-thrusts that involve the Apulian foreland plate underlying the now inactive thin-skinned accretionary wedge down to near-Moho depths. In light of the tight interlacing between regional and local components of deformation affecting the marine terraces, we suggest that the large-scale uplift in this sector of Calabria may reflect whole crustal-scale folding. The novel seismotectonic frame reconstructed for this region is consistent with GPS velocities suggesting that large part of geodetic shortening detected between the Apennines and the Apulian block on the eastern side of southern Italy might be accommodated in northern Calabria.

© 2008 Elsevier B.V. All rights reserved.

1. Introduction

The four-dimensional analysis of crustal deformation is notoriously difficult, largely due to the fact that modes and rates of deformation can be established with variable uncertainty depending on the time scale of observation. A mounting body of evidence is pointing to precise and accurate determination of the intermediate-scale (10 to

100 Ka) displacement pattern as vital in order to bridge the gap between tectonic events occurring at geologic (1 Ma) and historical (1 ka or less) time-scales (e. g. Friedrich et al., 2003). Whereas deformation processes occurring at the million-yr timescales have left their record in the vast majority of Cenozoic mountain belts, contemporary orogenic deformation is well depicted by seismicity and Global Positioning System (GPS) velocity analysis, but the two processes are not always reconciled with ease. The issue is of paramount importance in active orogens with relatively low displacement rates, where a straightforward comparison between the geological record and

* Corresponding author.

E-mail address: luigi.ferranti@unina.it (L. Ferranti).

the current deformation pattern supplied by geodesy and seismicity is often hindered by the subdued development of intermediate-scale markers of deformation.

These difficulties are typified by the Apennines orogen in southern Italy, where Neogene migration toward the Adriatic–Apulian foreland of paired contractional and extensional belts documented by stratigraphic and tectonic analysis (Fig. 1; Patacca et al., 1990; Monaco et al.,

1998; Menardi-Noguera and Rea, 2000; Van Dijk et al., 2000) contrasts with the modern deformation pattern highlighted by seismicity and active fault studies, which indicate dominant hinterland extension (Fig. 2). Migration of the deformation fronts evolved during westward subduction and roll-back of the Adriatic–Ionian slab (Fig. 1; Malinverno and Ryan, 1986; Patacca et al., 1990), but large uncertainties surround the source and pattern of current orogenic deformation in

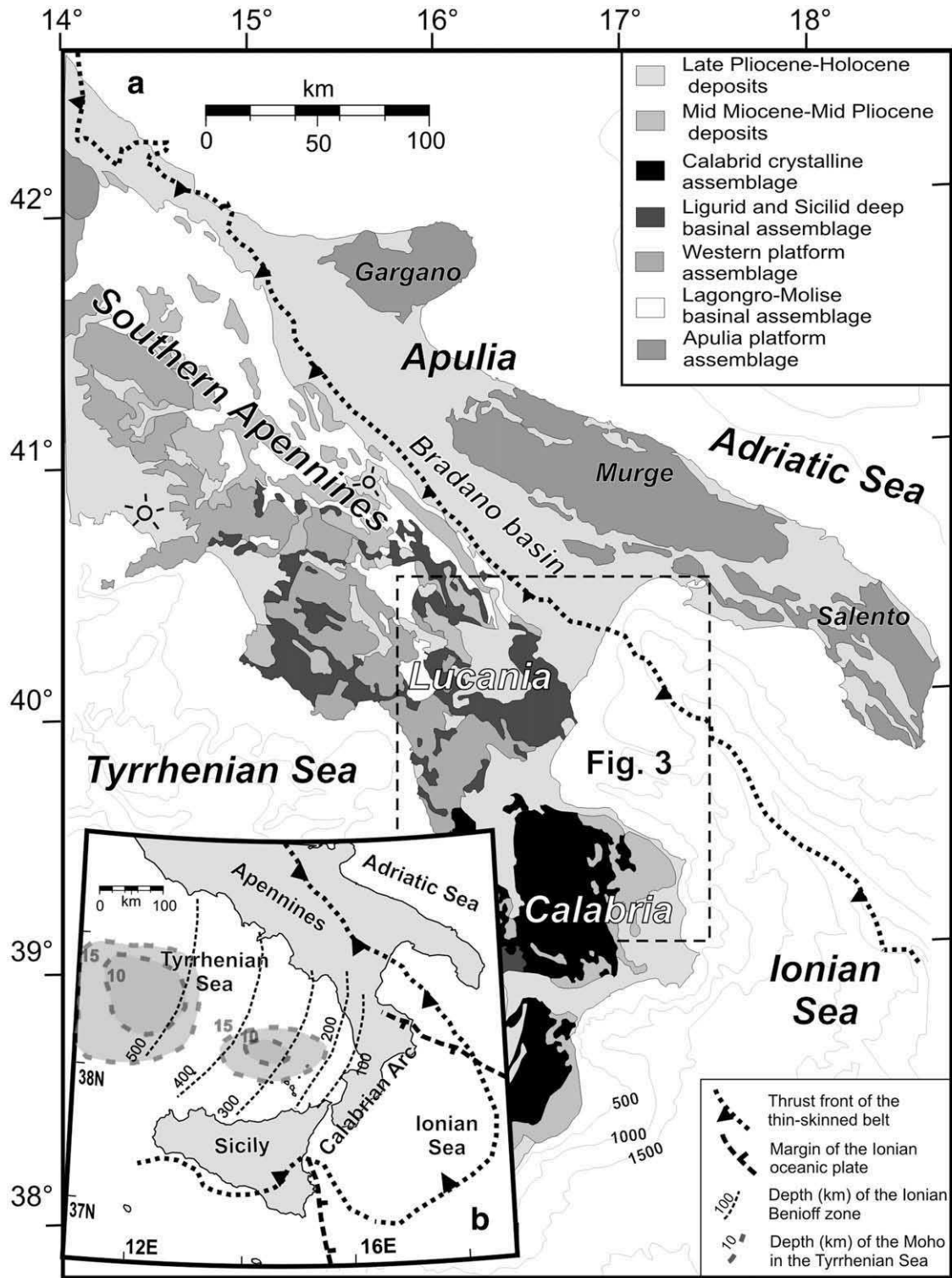


Fig. 1. (a) Regional setting of southern Italy showing the main lithotectonic assemblages of the Southern Apennines and Calabrian arc, and the front of the thin-skinned thrust belt (after Bigi et al., 1992). (b) Plate tectonic setting of southern Italy, showing the Benioff–Wadati zone of the Ionian slab (redrawn after Ferranti et al. (2007)), the parts of the Tyrrhenian Sea with Moho shallower than 15 and 10 km (after Cassinis et al., 2003), and the margins of the Ionian oceanic plate (after Catalano et al., 2001).

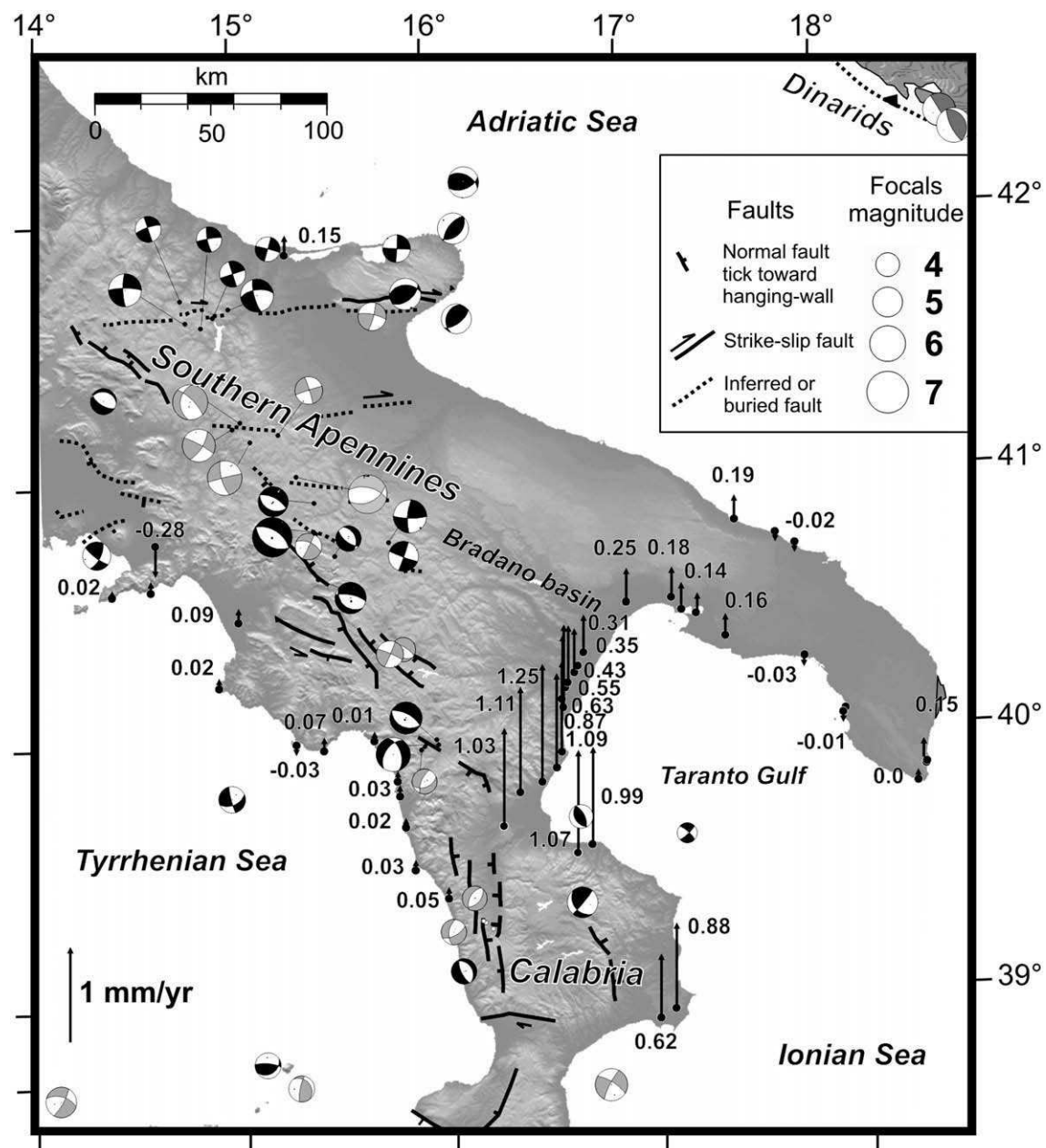


Fig. 2. Active deformation in southern Italy. Active faults (barbs on downthrown side) after Monaco and Tortorici (2000), Ferranti and Oldow (2005), and the DISS database (<http://legacy.ingv.it/DISS/>). Focal mechanisms of $M > 4$ crustal earthquakes after Harvard CMT [1976–2007] (<http://www.seismology.harvard.edu/CMTsearch.html>) and Mednet RCMT [1997–2007] (<http://mednet.ingv.it/events/QRCMT/Welcome.html>) catalogues (black), Gasparini et al. (1985; light grey), and Anderson and Jackson (1987; heavy grey). Arrows show the vertical displacement rate (mm/yr) of the 124 ka marine terrace (after Ferranti et al., 2006).

southern Italy. According to many investigators, a geodynamic change has occurred in the region during the Middle Pleistocene, and is signaled by the end of frontal thrust displacement and stalling of subduction (Fig. 1; Hippolyte et al., 1994; Patacca and Scandone, 2001; Goes et al., 2004).

On the Ionian Sea coast of southern Italy, straddling the frontal thrust belt of the Apennines, Middle Pleistocene and younger marine terraces were uplifted at average rates which peaked at over ~ 1 mm/yr on the coastal projection of the mountain chain (Fig. 2; Westaway, 1993; Bordoni and Valensise, 1998; Ferranti et al., 2006). Since horizontal motion of the thrust front in the Southern Apennines reportedly ended by the late Early Pleistocene (Patacca and Scandone, 2001), and the active extensional belt has not encroached on this region yet, the vertical displacement is commonly attributed to the deep-seated, regional uplift of the Calabrian arc (Bordoni and Valensise, 1998; Cucci and Cinti,

1998). On the other hand, analysis of long-term orogenic displacement suggests that a contribution to Quaternary uplift in the frontal zone and foreland of the Southern Apennines was provided by distributed deep-seated thrusting (Ferranti and Oldow, 2005) and/or lithospheric folding (Bertotti et al., 2001), a pattern that may be reflected in current horizontal motion provided by GPS velocity fields (Oldow and Ferranti, 2006; Ferranti et al., 2008).

In order to improve understanding of the complex Quaternary displacement field in the region, we present results of a structural and geomorphologic study of the frontal thrust belt centered on the Ionian Sea coastline of northern Calabria (Fig. 3). Our integrated analysis reveals that uplift of Middle Pleistocene and younger marine terraces not only ensues from a regional-scale process, but also reflects a smaller-wavelength component of shortening which, as this study will show, can be attributed to local tectonic structures. The tight coupling between local and regional-

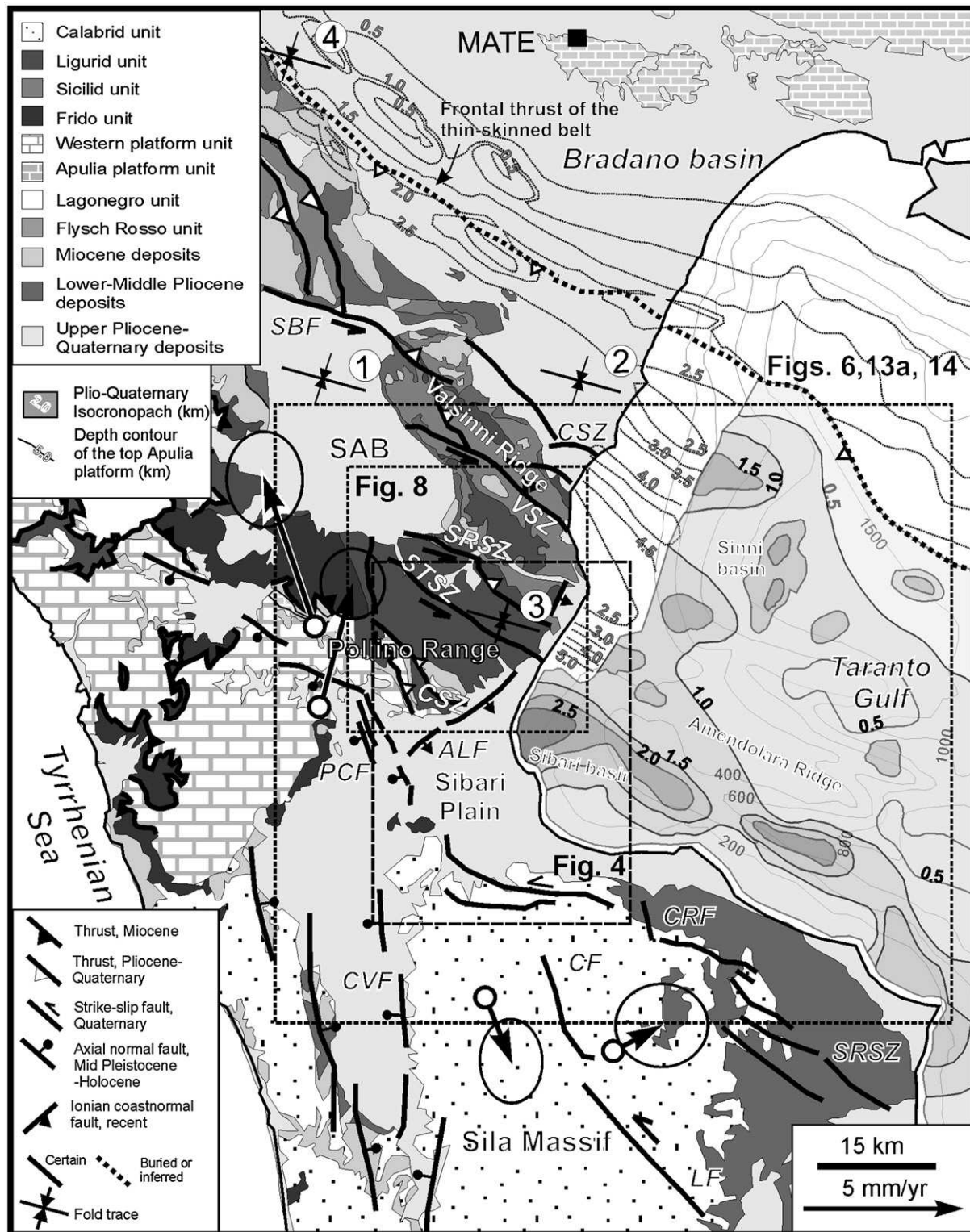


Fig. 3. Tectonic map of the Southern Apennines in southern Lucania and northern Calabria. Active normal faults in the mountain chain as in Fig. 2; strike-slip faults in northern Sila after Galadini et al. (2000) and Galli and Bosi (2003); strike-slip faults in the Pollino range after Catalano et al. (1993). Other faults and geology after Bigi et al. (1992). Recent folds after: (1) Casciello et al. (2000); (2) Bianca and Caputo (2003); (3) Cesarano et al. (2002); (4) Pieri et al. (1997). Arrows show GPS velocities (1995–2000) residuals to MATE from sites of the PTGA array (after Ferranti et al., 2008). Apulian platform depths and isochronopach of Pliocene–Quaternary deposits after Bigi et al. (1992). Faults: CF, Cecita fault; CRF, Corigliano–Rossano fault; CSZ, Canna shear zone; CVF, Crati Valley fault; CVSZ, Civita shear zone; LF, Lake fault; PCF, Pollino–Castrovillari fault; SBF, Scorciabuoi fault; SCSZ, Saraceno shear zone; ALF, Avena–Laupoli fault; SRSZ, San Nicola Rossano shear zone; STSZ, Satanasso shear zone; VSZ, Valsinni shear zone. SAB, Sant’Arcangelo basin.

scale deformation carries the important implication that surficial and deep structures may be linked, and thus shortening may contribute to regional uplift in this part of the Calabrian arc.

Besides helping to reconcile deformation patterns at different time-scales, resolution of the mode and magnitude of crustal motion partitioning into local and regional components contributes to the

understanding of active tectonic structures and places constraints on models of Calabrian arc–Southern Apennines kinematics.

2. Tectonic background

2.1. Regional setting

Growth of the Apennines and Calabrian arc orogens in southern Italy occurred during Neogene north–westerly subduction and easterly roll–back of the Adriatic–Ionian slab (Malinverno and Ryan, 1986; Gueguen et al., 1998; Faccenna et al., 2001). Today, the slab is imaged by seismic tomography and by deep earthquakes beneath the south-eastern Tyrrhenian Sea (Fig. 1b; Selvaggi and Chiarabba, 1995; Wortel and Spakman, 2000). Regional geophysical studies (Catalano et al., 2001 and references therein) show that the deep transition from the Adriatic continental crust to the Ionian thinned continental or oceanic crust occurs beneath the study region in northern Calabria (Fig. 1b).

Deformation in southern Italy swept from west to east across the western Adriatic continental margin as crystalline, basinal and carbonate platform rocks were incorporated as thrust imbricates within the growing orogen (Fig. 1a). The Southern Apennines includes two vertically superposed contractional belts (Casero et al., 1992; Menardi-Noguera and Rea, 2000; Patacca and Scandone, 2001). The upper belt formed in response to Late Oligocene to Early Pleistocene shortening, and includes Paleozoic–Mesozoic crystalline and deep basinal rocks structurally overlying Mesozoic–Tertiary platform carbonates and basinal rocks (Fig. 1a). These pre-orogenic rock assemblages are unconformably covered by Oligocene–Quaternary terrigenous deposits, which were deposited in migrating foreland and piggy-back basins (Fig. 1a; Patacca et al., 1990; Van Dijk et al., 2000). The lower thrust belt involves Mesozoic–Tertiary carbonates which represent the western extension of the Apulian platform rocks exposed to the east, and buried beneath the upper thrust belt as documented by seismic reflection profiles and oil exploration wells (Fig. 3; Roure et al., 1991; Casero et al., 1992; Menardi-Noguera and Rea, 2000; Patacca and Scandone, 2001). The southward termination of the buried Apulian rocks in northern Calabria coincides with the transition between continental and thinned/oceanic crust (Fig. 1b).

Shortening was marked by a complex history of tectonic transport resulting in non-coaxial superposition of structures (Monaco et al., 1998; Cello and Mazzoli, 1999), and its timing is constrained by synorogenic sequences exposed in the thrust belt or recovered by exploratory wells above the buried Apulian platform. Motion of the thin-skinned thrust front in the Southern Apennines ceased during Early Pleistocene as the front was buried beneath the western margin of the Bradano foredeep basin (Fig. 1a; Patacca and Scandone, 2001). Contraction in the Apulian belt beneath the Apennines is thought to have commenced during the Pliocene, and during Early Pleistocene was manifested by transpressional faults breaking through the previously emplaced thin-skinned allochthon (Knott and Turco, 1991; Catalano et al., 1993; Monaco et al., 1998; Van Dijk et al., 2000; Tansi et al., 2007). At present, shortening in the Apulian belt is thought to have ceased, and limited transpression occurring in the northern part of the Apulia block is attributed to Africa–Europe plate interaction (Fig. 2; e.g. Montone et al., 2004).

Since ~10 Ma (Malinverno and Ryan, 1986; Gueguen et al., 1998; Faccenna et al., 2001), extension within the hinterland of the orogen stretched continental crust and resulted in the local formation of oceanic crust beneath the southern Tyrrhenian Sea (Fig. 1b). Extension is typically regarded as a back-arc spreading process above the retreating slab (Malinverno and Ryan, 1986; Faccenna et al., 2001), and it has progressively encroached within the mountain belt. Today, an array of active normal faults is traced along the axis of the Apennines (Fig. 2). The extension direction determined by fault slip analysis (Hippolyte et al., 1994; Monaco and Tortorici, 2000; Maschio et al., 2005), focal mechanisms of crustal earthquakes (Harvard and Mednet

CMT Catalogues) and GPS geodetic velocities (Hunstad et al., 2003; Ferranti et al., 2008) trends ~NE–SW in the Apennines and ~E–W in northern Calabria (Fig. 2). Regional GPS velocity fields point to a reduction in the rate of Ionian slab retreat and Tyrrhenian back-arc extension with respect to the geologic rates, but whether subduction is ongoing is debated (Oldow et al., 2002; Hollenstein et al., 2003; D'Agostino and Selvaggi, 2004; Goes et al., 2004).

Whereas active extension in the mountain belt is well documented by fault-plane solutions of crustal earthquakes and active fault studies, the current seismotectonic frame of the southern Apulia block and of the frontal belt in southern Lucania and northern Calabria is poorly understood due to the lack of significant seismicity and poor expression of active faulting (Fig. 2). In contrast with the hinterland side, however, the frontal belt has experienced dramatic uplift since Middle Pleistocene (Fig. 2). Uplift is spectacularly documented by flights of coastal terraces and wave-cut platforms displaced to hundreds of meters above the present sea-level (e. g. Westaway, 1993; Miyauchi et al., 1994). In particular, well-developed and preserved markers of the last interglacial period, equated to the Marine Isotope SubStage (MIS) 5.5 and dated at ~124 ka, provide the best constraint to evaluate the regional uplift pattern (Fig. 2; Ferranti et al., 2006). Uplift is viewed as an isostatic (Westaway, 1993; Wortel and Spakman, 2000) or dynamic (Gvirtzman and Nur, 2001) response to removal of a high-density deep root, or, alternatively, as arising from trapping of Calabria between buoyant continental landmasses in Apulia and in southern Sicily (Fig. 1b; Goes et al., 2004). Backstripping analysis of foredeep sedimentary patterns in the southern Adriatic Sea suggests that a component of large-scale folding rooted at deep crustal and perhaps lithospheric levels may have contributed to uplift (Bertotti et al., 2001). This analysis is consistent with the regional pattern of Quaternary uplift, that involved the whole Apulian block and may embed a component of deep shortening not directly related to slab dynamics (Ferranti and Oldow, 2005).

2.2. Tectonic frame of the Ionian Sea sector of the frontal belt

The study area lies behind the thin-skinned thrust front of the Southern Apennines in southern Lucania and northern Calabria (Fig. 1). In this region, the geological architecture consists of Paleozoic crystalline rocks and related Mesozoic–Cenozoic forearc sediments of the Calabrid units which outcrop to the south in the Sila massif, and of Mesozoic–Cenozoic sedimentary rocks of the Apenninic platform and of the Ligurid and Sicilid basins, which are found in the Pollino mountain range to the north (Fig. 3). Following Late Oligocene–Pliocene assembly of these tectonic units (Bonardi et al., 2001; Patacca and Scandone, 2001), the area was filled by Uppermost Pliocene? to Lower Pleistocene marine terrigenous deposits (Colella and Cappadona, 1988), and by Middle Pleistocene to Holocene marine and continental deposits (Westaway, 1993; Cucci and Cinti, 1998; Cucci, 2004).

The pristine Miocene–Pliocene low-angle tectonic contacts between crystalline and sedimentary rocks have been sliced by Quaternary high-angle strike-slip and extensional faults (Fig. 3). The Pollino–Castrovillari normal fault borders to the southwest the Pollino range and displays paleoseismological evidence of activity (Cinti et al., 1997). The fault system projects to the south across the high reach of the Sibari plain to merge with the seismically active normal faults at the eastern part of the Crati Valley (Figs. 2 and 3). Thus, the belt of active extension in the axial sector of the Apennines is confined to the west of the Sibari plain and Pollino and Sila mountain ranges.

The northern side of the Sila massif is bordered by the WNW-striking Corigliano–Rossano fault, which acted as left-lateral during the Pliocene–Quaternary, and whose present activity is debated (Galadini et al., 2000; Cucci, 2004). Detailed geomorphic analysis shows evidence of recent motion along this faults system, which is

thought to slip as normal (Molin et al., 2004). Evidence of left strike-slip motion is found on other NW–SE striking faults both on-land (San Nicola–Rossano shear zone, Van Dijk et al., 2000; Tansi et al., 2007) and offshore (Sibari fault, Del Ben et al., 2007). To the south, in the interior of the Sila block, paleoseismological evidence of left strike-slip is reported on the Cecita and Lake faults (Galli and Bosi, 2003).

The northwestern side of the Sibari plain is bound, according to some investigators, by a ~NE-striking fault system, here named Avena–Lauropoli fault (Fig. 3). Although listed in some fault map compilations as a dip-slip extensional structure (Lanzafame and Tortorici, 1981; Ambrosetti et al., 1987; Bigi et al., 1992), the existence and recent activity of the fault has been questioned by others (Cucci, 2004).

Behind the buried trace of the thin-skinned thrust belt in the Bradano basin, the Pollino range is sliced by sub-parallel arrays of ~NW–SE striking faults (from south to north: Civita, Satanasso, Saraceno, Valsinni and Canna shear zones, Fig. 3), showing evidence of left transpressional slip during the Early and possibly the Middle Pleistocene (Catalano et al., 1993; Monaco et al., 1998). These structures replaced motion of the thrust front as a result of involvement in shortening of the thick Apulian crust (Catalano et al., 1993; Monaco et al., 1998).

The Civita shear zone bounds the Pollino range at its south-eastern border, where the active Pollino–Castrovillari normal fault terminates (Fig. 3). The Saraceno shear zone forms the northern boundary of the Pollino range at the transition with the Late Pliocene–Middle Pleistocene Sant’Arcangelo thrust-top basin (Fig. 3). The Canna shear zone and Valsinni shear zone define the NNW-trending Valsinni ridge, that bound to the northeast the Sant’Arcangelo basin. Growth of this ridge at the end of the Early Pleistocene is thought to have caused the latest shortening in the basin (Hippolyte et al., 1994; Patacca and Scandone, 2001).

A marked component of shortening is manifested by thrusts and folds associated to the main left-lateral arrays, and might be associated to the younger generation of folds (Fig. 3) found both in the Miocene bedrock (Cesarano et al., 2002) and in Early–Middle Pleistocene deposits which fill the Sant’Arcangelo thrust-top basin (Casciello et al., 2000) and the northern side of the Sibari plain (Hippolyte et al., 1992). Scant geomorphic and structural evidence of post-Middle Pleistocene shortening has been reported along the front of the Southern Apennines (Fig. 3; Pieri et al., 1997; Bianca and Caputo, 2003), but rates and patterns of this recent contraction are still unclear.

Global Positioning System (GPS) velocities of sites of the Pery-Tyrrhenian Geodetic Array (Ferranti et al., 2008), when viewed with respect to the IGS site MATE in the north (Fig. 3), are consistent with structural evidence of recent deformation in the region. Within the Sila range, two sites straddling the Cecita and Lakes faults, have ~2 mm/yr left-oblique differential motion, consistent with paleoseismological estimations (Galli and Bosi, 2003). Likewise, two GPS sites straddling the Pollino–Castrovillari fault at the southern border of Pollino have a residual velocity that suggests ongoing left transtensional displacement across the fault at ~2 mm/yr. This estimate is broadly consistent with the Holocene (~1 mm/yr; Cinti et al., 1997) and Pleistocene (3–4 mm/yr; Colella and Cappadona, 1988) estimates of fault slip. Notably, the two sites at Pollino move toward MATE indicating that at least 5 mm/yr shortening is accommodated between MATE and Pollino (Fig. 3). Similarly, the eastern GPS site in the Sila range converges obliquely toward MATE, and thus left transpression on the Corigliano–Rossano and S. Nicola–Rossano faults is feasible (Fig. 3).

Seismic reflection profiles in the Taranto Gulf attest the offshore extension of the structures mapped on-land. The offshore projection of the Pollino morphostructural culmination coincides with the prominent bathymetric high of the Amendolara ridge, which to the west swings northward to join with the Valsinni ridge (Fig. 3). Offshore the Sibari plain, a large depocenter filled by >2.5 km of Pliocene–Quaternary deposits is imaged in the Sibari basin (Fig. 3). To

the east, this narrow and elongated basin turns southward and parallels the steep submarine scarp of the Amendolara ridge.

Marine geophysical data support recent and possibly active transpression and folding. Seismic reflection profiles across the Sibari basin and Amendolara ridge (Del Ben et al., 2007), show that the Miocene–Pliocene thrust belt is cut by steeply-dipping transpressional faults. Whereas the Sibari basin is suggested to be located above a deep-seated strike-slip fault (Sibari fault), a marked positive structure involving large part of the Quaternary sedimentary package is located beneath the Amendolara ridge (Del Ben et al., 2007).

2.3. Uplift and deformation of marine terraces

Flights of Middle–Late Pleistocene marine terraces are found along the Ionian coastline of northern Calabria, and were carved either in pre-Pleistocene bedrock or in Early Pleistocene marine deposits. Following decades of detailed geomorphic and sedimentological analysis mostly centered north of Pollino (Dai Pra and Hearty, 1988; and references therein), uplifted marine terraces in the study area were more recently studied by Cucci and Cinti (1998), who mapped 7 terraces along the eastern side of the Pollino range between 12 and 420 masl. Mapping of terraces was extended to the south across the Sibari plain by Cucci (2004), who found 5 strandlines at elevations between 60 and 650 m.

Lateral correlation with radiometrically dated terraces in the Bradano foredeep to the north allowed Cucci and Cinti (1998) to assign the Pollino terraces to as many Middle Pleistocene (~600 ka) to Holocene highstands of the global sea-level curve. In later work by Cucci (2004), the second terrace from the bottom (T2) was assigned to the MIS 5.5 and aged at 124 ka based on amino acid racemization on shells retrieved from locally preserved terrace deposits. Following earlier proposition by Westaway (1993), terrace uplift at ~1 mm/a during the last ~600 ka was attributed by Cucci and Cinti (1998) and Cucci (2004) to a regional source. Minor differential displacement of the terrace flight was attributed to footwall uplift caused by slip on the Pollino–Castrovillari fault. Conversely, no evidence of terrace offset was found across the Avena–Lauropoli and Corigliano–Rossano faults.

North of the Pollino range, terraces uplift in the Bradano basin decreases to a minimum at the northern shore of the Taranto Gulf (Fig. 2). No significant jump in the regional uplift pattern is observed crossing the front of the thin-skinned thrust belt (Figs. 2 and 3), supporting the notion that large horizontal displacement had vanished by onset of the Middle Pleistocene (Patacca and Scandone, 2001). Although most investigators mapped flights of Quaternary terraces in the Bradano basin (Dai Pra and Hearty, 1988; Westaway, 1993; Amato and Montone, 1997; Westaway and Bridgland, 2007), Bentivenga et al. (2004a,b) proposed the existence of a single Middle Pleistocene terrace cut by extensional faults that displace toward the Ionian Sea. According to Bentivenga et al. (2004a,b) development of this Ionian-dipping fault system would be related to large-scale gravitational processes triggered by the regional SE-ward tilting of the Bradano basin.

3. Geomorphologic and structural markers of deformation

3.1. Displaced coastal terraces

3.1.1. Methods

Marine terraces were mapped in detail using aereophotography and extensive field work, which allowed to compute uncertainties in elevation of their inner margin on a site-by-site basis. Particular care was devoted to apply a sequential correction to the measured elevations in order to retrieve the nominal paleo-shoreline elevation, as briefly outlined in the following.

Uncertainty in elevation estimates of the inner edges of the marine terraces stems from a combination of accuracy in marker identification

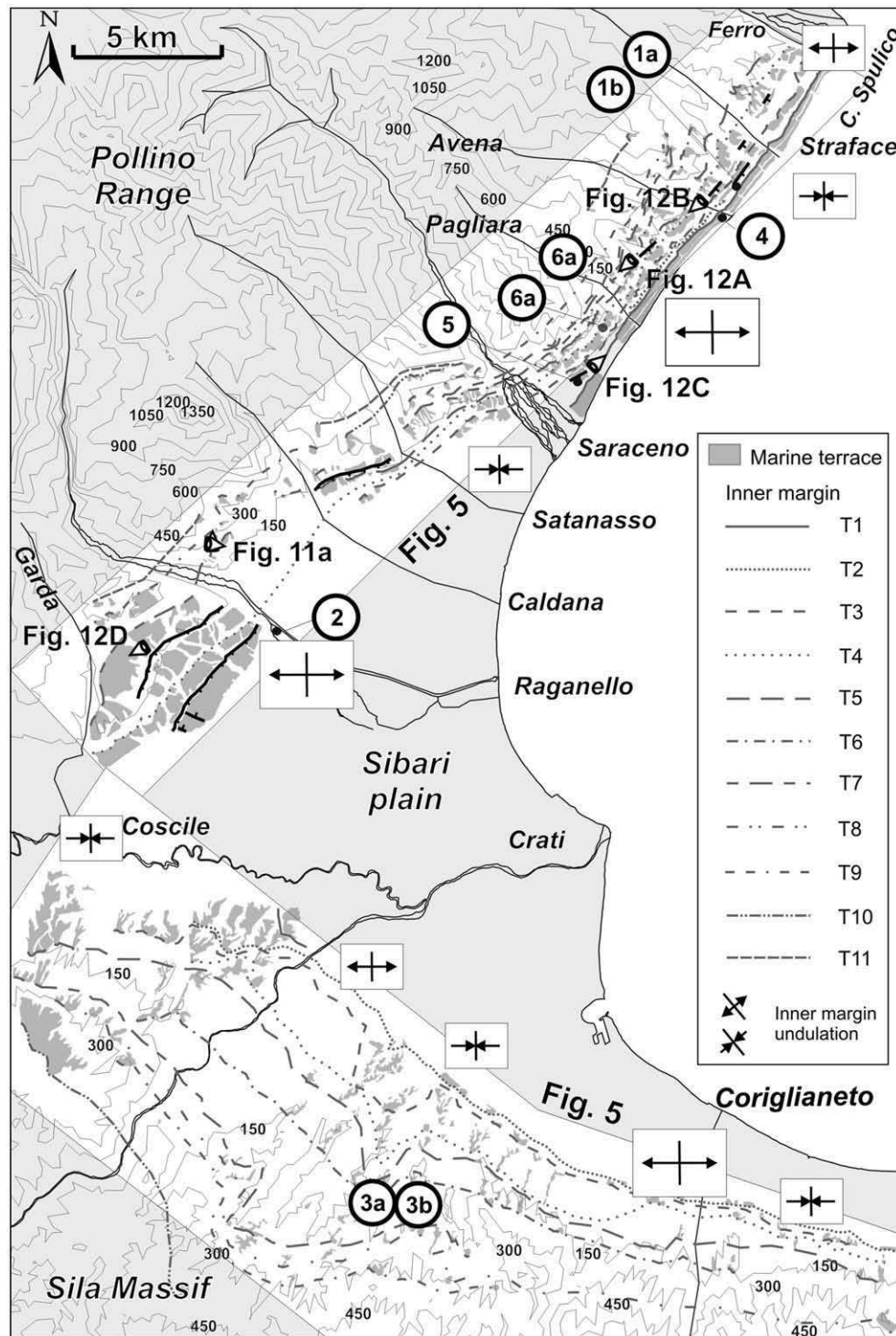


Fig. 4. Map of Middle Pleistocene–Holocene marine terraces on the Ionian Sea coast of northern Calabria, showing the trace of the inner edges and the generalized location of main positive and negative undulations in the uplift profile (see Fig. 5). Heavy lines are normal faults of the Avena–Laupoli system cutting the terraces. Large boxes framing the terraces are generalized swaths used for construction of terrace elevation profiles in Fig. 5. Circled numbers refers to samples listed in Table 2.

and precision in measurement. The 1:5000 scale maps used to trace the inner edges, have 10-m and locally 5-m contours. Thus, uncertainty in elevation estimate is probably within 10 m. Handheld GPS and altimeters used to retrieve spot location of inner edges have a similar 10 m uncertainty.

The following correction was intended to retrieve the elevation of marine deposits or forms from the observed inner margins, the two measured values being commonly different due to accumulation of

more recent continental cover following emergence of the terrace. The thickness of sedimentary covers shedding the terrace inner edges is highly variable but is commonly < 10 m. Thus a +5/–15 m maximum uncertainty in elevation estimation of marine depositional/erosional markers is reliable.

The largest uncertainty arises from ambiguity in paleo sea-level correction for different markers, which was evaluated at individual locations following estimates stipulated in Ferranti et al. (2006).

Finally, we applied a minor correction accounting for the missing identification of coastal onlaps and shoreline angles by projecting the topmost identified marker (both depositional/erosional) at each location toward the paleo-sea cliff.

A complete discussion of the sedimentological, morphometric and geochronological features the terrace flight is presented in a companion paper (Santoro et al., in press on Quaternary International, hereinafter Santoro et al., 2009). Following Santoro et al. (2009), the main morphologic features of the terraces are summarized below, with the focus being placed on the vertical displacement and deformation profile of terraces.

3.1.2. Present elevation of uplifted paleo-shorelines

Detailed mapping and correlation of individual terrace remnants allowed to identify eleven terrace orders, plus a lowermost, Holocene terrace, which are scattered at elevations of between ~5 and ~480 masl. (Fig. 4 and Table 1). Higher remnants were recognized up to ~650 m (Cucci, 2004), but due to the very sparse distribution and difficulty in correlation, they were discarded from further analysis. In spite of the marked morphological difference between the northern and southern sectors, where the flanks of the Pollino and Sila ranges plunge steeply into the Ionian Sea, and the central sector represented by the large aggradational engulfment of the Sibari plain, the eleven terrace orders can be laterally correlated. The transition between northern and southern sectors coincides with the Coscile stream, where the orientation of the present and paleo-coastlines turns from NE-SW in the north to NW-SE in the south (Fig. 4).

Profiles of the paleo-shoreline elevation drawn parallel to the present and the ancient coastlines allow appreciation of both the total and the differential uplift accrued by the Pleistocene terraces (Fig. 5). The compound profile was constructed by projecting the estimated elevation of each terrace across two swaths parallel to the two arms of the embayment, from SE to NW in the south and from SW to NE in the north. Based on the high number of control points on past shoreline position and the admissible error on elevation estimate, a well constrained reconstruction of their present shape has been afforded (dashed line fitting through data-points, Fig. 5). Elevations given in text refers to the fitting point and will be rounded for simplicity to the nearest 5 m (precise elevations are in Table 1). Note that in the largest number of cases the fitting line crosses the middle of the error bar. Only in few instances the fitting line has been manually shifted along the bar to allow geometric consistency with the deformation profile of the remaining terraces at that specific locations.

At the Pollino coast, the lowermost Pleistocene terrace, T1, is covered by the narrow strip of the modern coastal plain, but a distinct inner margin can be traced against a continuous ~10 m high paleo-cliff at elevations which increase to the south from ~10 to ~25 m (Figs. 4 and 5). By contrast, only scattered outcrops of T1 are found in the south.

Terraces T2 and T3 are represented by small remnants at elevations which increase southward along the Pollino coast from ~35 to ~65 m and from ~60 to ~95 m, respectively (Fig. 5, Table 1). In the Sibari plain, mapping of T2 and T3 is difficult due to the thick aggradational cover, but on the Sila border the two terraces are again mapped at an elevation comparable to that attained in the north (Fig. 5, Table 1). Previous workers mapped only the upper terrace at broadly similar elevations in the Pollino range (T2 of Cucci and Cinti, 1998; Table 1) and Sibari plain to Sila (T1 of Cucci, 2004), but failed to recognize our T2 terrace. This terrace is very narrow at the Pollino coast but reaches a substantial width at the Sila coast (Randisi, 2007; Santoro et al., 2009). In addition, the marine origin of terrace T2 is supported by the lateral continuity of remnants (Fig. 4) and the local finding of ~15 m thick marine deposits on the terrace (Santoro et al., 2009). As clearly shown in Fig. 5, short-wavelength undulations can be detected in the coast-parallel profile of T2 and T3, a pattern which persists for the higher terraces. The lower elevations of these terraces in the north between the Avena and Ferro streams partly results from displacement along small, en echelon normal fault strands which are superposed to the undulated profile (Figs. 4 and 5).

Terrace T4 is by far the widest within the terrace flight (Fig. 4), a feature that allowed a robust lateral correlation of remnants across different sectors. Along the Pollino coast, T4 rises southward from ~95 to ~125 m. The local undulations show a southward asymmetry, particularly in the area between the Saraceno and Avena streams (Fig. 5). In the Sibari plain, between the Satanasso and Coscile streams, the terrace is placed at a ~20 m lower elevation, but it rises again to ~100–130 m along the Sila hillslope (Fig. 5, Table 1).

Terrace T5 is less wide than T4, but it can be mapped continuously between ~120 and 185 m. The lower elevations are found in the central sector between the Raganello and Coscile streams, with the large scatter resulting from activity of a normal fault which drops the terrace down at this locale (Fig. 5). This terrace was mapped at a broadly similar elevation on the Pollino coast by Cucci and Cinti (1998; their T3), but in the Sibari plain and Sila slope it was incorporated with our T4 by Cucci (2004; his T2; Table 1).

T6 remnants, albeit of narrow size, were readily correlated across erosional ridges at an average elevation of ~180–225 m at the Pollino coast and between 160 and 200 m at the Sila slope (Fig. 5, Table 1). As observed for lower terraces, this order was mapped at comparable elevations in the north by Cucci and Cinti (1998), but went unrecognized in the south by Cucci (2004). Notwithstanding, it is clear that starting from T6 and keeping on with the overlying orders, a pattern of higher elevations is established at the southern border of the Pollino between the Coscile and the Satanasso streams (Fig. 5).

The impending orders are represented by strongly eroded and widely separated terrace remnants (Fig. 4). In addition, unlike the underlying terraces, marine deposits were totally stripped off from these higher terraces. Due to these limitations, lateral correlations of terrace remnants

Table 1
Marine terraces data in northeastern Calabria, and comparison with previous studies

This paper					Previous works			
Terrace order	Elevation, m		Marine isotope stage	Age ^a , ka	Cucci and Cinti, 1998 (Pollino)		Cucci, 2004 (Pollino and Sila)	
	Pollino	Sila			Terrace order (elevation, m)	MIS	Terrace order (elevation, m)	MIS
T1	11–24	17	3.3/3.1	61/40	T1 (12–20)	1		
T2	33–64	45–70	5.1	82				
T3	56–96	75–93	5.3	101	T2 (60–80)	5.1	T1 (60–80)	5.3
T4	94–123	103–130	5.5	124	T3 (85–135)	5.3	T2 (115–145)	5.5
T5	120–185	130–165	7.1	197	T4 (115–175)	5.5		
T6	180–225	158–196	7.3	215	T5 (170–235)	7		
T7	252–292	198–230	7.5	236	T6 (220–340)	9	T3 (220–260)	
T8	303–340	260–284	9.1	287				7
T9	363–415	343–365	9.3	313			T4 (340)	9
T10	398–448	385–393	9.5	331	T7 (420)	15		
T11	437–486	440–445	11	407				

^a After Waelbroeck et al. (2002), and Bassinot et al. (1994).

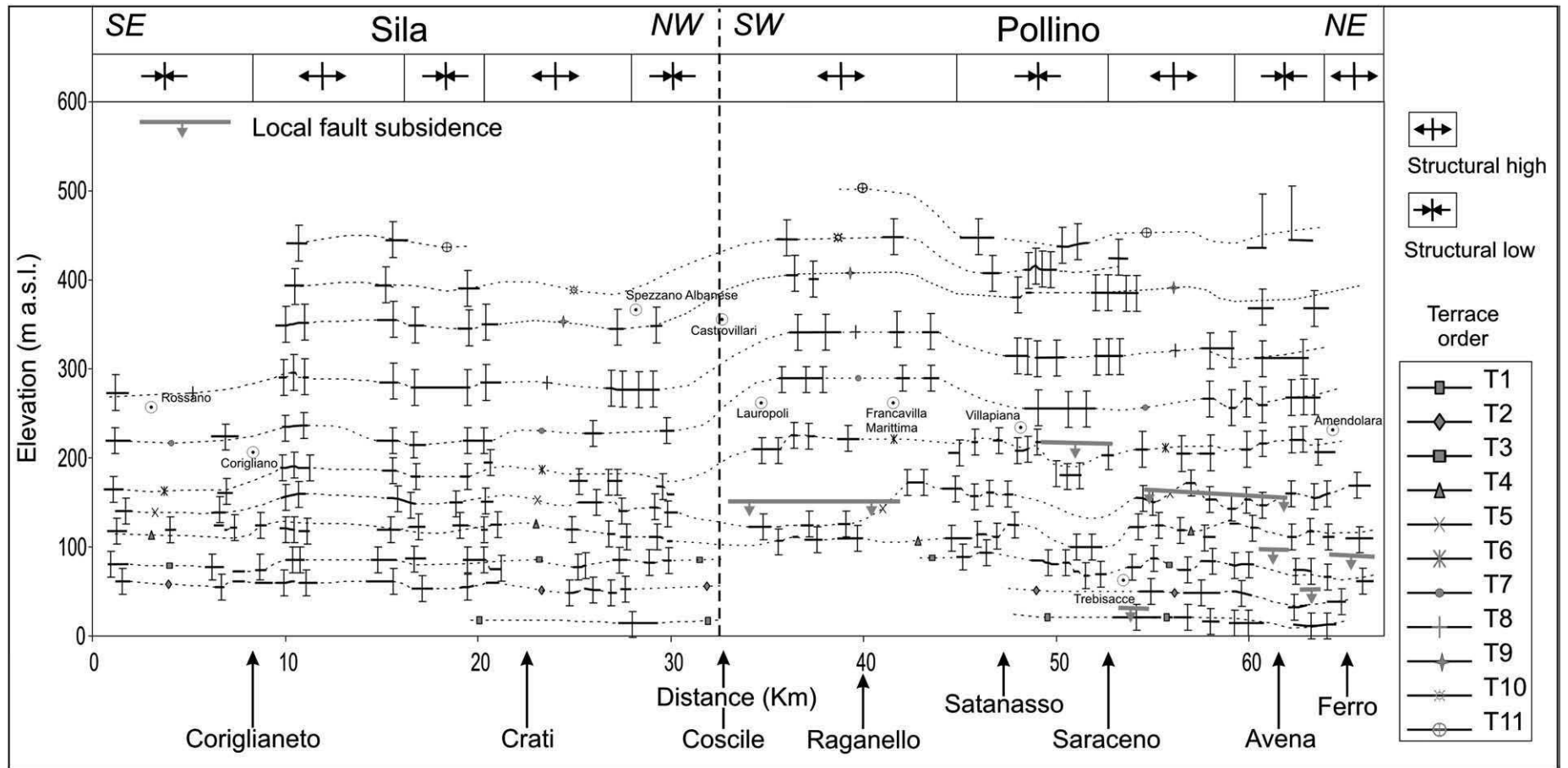


Fig. 5. Coast-parallel profiles of the inner edge of Middle Pleistocene–Holocene marine terraces in northeastern Calabria. Top panel shows positive and negative undulations in the uplift profile. Note that the profile runs NE–SW and NW–SE to the south and the north, respectively, of the Coscile stream (see Fig. 4).

Table 2
New and existing radiometric data for marine terraces in northeastern Calabria

No.	Field-code	Lab number	Elevation (masl)	Shell	Coordinates	Locality	Age (ka ± ka)	Terrace provenance	Field position	Attribution
1a	J2A	K-5313	23	<i>Cardium</i> sp.	N39°55'13.0" E16°35'08.7"	Tarianni	162 ± 12 ^a	T2	Resedimented	MIS 6 (6.5)
1b	J2A	K-5313a	23	<i>Cardium</i> sp.	//	Tarianni	98 ± 10 ^a	T2	Resedimented	MIS 5 (5.3)
2	97	K-53553B	53	<i>Chlamys</i> sp.	N39°46'24.06" E16°23'19.21"	Lauropoli	262 ± 46 ^a	T4	Resedimented	MIS 7–8–9 (7.3/7.5/8/9.1)
3a	128	K-5355A	125	<i>Cardium</i> sp.	N39°36'39.66" E16°26'44.65"	Vaccarizzo Albanese	135 ± 20 ^a	T4	In place	MIS 5 (5.5)
3b	128	K-53553b	125	<i>Cardium</i> sp.	//	Vaccarizzo Albanese	202 ± 16 ^a	T4	Resedimented	MIS 7 (7.1–7.3)
4	J14	Poz-21913	2.5	<i>Cardium</i> sp.	N39°54'33.2" E16°34'47.9"	Avena	40 ± 0.4 (Cal 44 ± 0.39) ^b	T1	Resedimented	MIS 3 (3.1)
5	J10bis	K-5316	25	Shell	N39°51'39.92" E16°31'21.56"	Trebisacce	~ 130	T3	Resedimented	MIS 5.5
6a	–	–	114	<i>Glycymeris</i> sp.	N39°52'39.92" E16°31'54.56"	Trebisacce	130 ^c	T4	In place	MIS 5 (5.5)
6b	–	–	65	<i>Glycymeris</i> sp.	N39°52'17.33" E16°31'53.32"	Trebisacce	139 ^c	T3	Resedimented	MIS 5 (5.5)

^a Electron Spin Resonance age performed at the University of Cologne, Germany.

^b Radiocarbon age performed at Poznan Radiocarbon Lab, Poland. Calibration used the Fairbanks 0805 Calibration curve (Fairbanks et al., 2005).

^c Predicted age from amino acid racemization value from Cucci (2004).

proved difficult, and mostly relayed on elevation criteria constrained by the deformation profile of subjacent, better correlated terraces.

Whereas T7 is represented by very few remnants between ~250–290 m in the north and ~200–230 m in the south, T8 can be traced with larger confidence between ~300–340 and 260–285 m within the two sectors, respectively (Fig. 5, Table 1). Only very sparse remnants are found at the Pollino coast for terraces T9 (~365–415 m), T10 (~400–450 m) and T11 (~435–485 m). By contrast, these terraces are better developed and preserved on the Sila slope at consistently lower

elevations (Table 1). Whereas terraces T7 to T9 at the Pollino coast were mapped as a single order by Cucci and Cinti (1998), they were later distinguished by Cucci (2004) in the southern sector (Table 1, with the notable lack of our T8). Regarding the uppermost terraces, only T10 was mapped by Cucci and Cinti (1998) at the Pollino slope (Table 1).

3.1.3. Terrace age

Few chronological constraints exist on the terrace flight. Northward extrapolation of terrace T4 would join this order to a terrace lying at

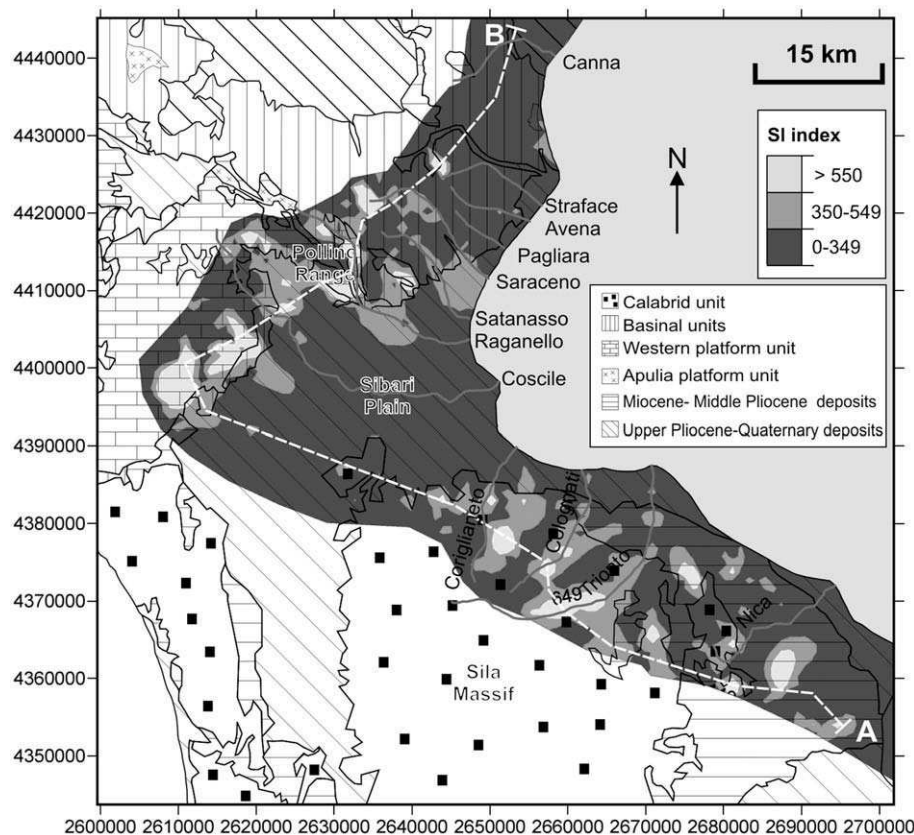


Fig. 6. Contour map of the Stream-Length ratio index showing the distribution of anomalies. Main streams are indicated by solid lines. Generalized geology as in Fig. 3.

~115 m elevation on the southern flank of the Bradano basin (just south of the Canna shear zone, Fig. 3), which was attributed to the MIS 5.5 at ~124 ka based on radiometric analysis of shells from the underlying terrace (Dai Pra and Hearty, 1988; Amato and Montone, 1997). This correlation was confirmed by Cucci (2004), who assigned a MIS 5.5 age to our T4 (his T2) terrace based on amino acid geochronology.

In order to add further constraints on terrace age attribution, Electron Spin Resonance (ESR) and AMS ^{14}C dating was conducted on shells collected from different terraces (Table 2, which includes data from Cucci, 2004). Details of methods and results are provided by Santoro et al. (2009) and are here summarized. The chronological attribution of the terrace flight as constrained by dating is listed in Table 1, where major and minor highstands which occurred in the last ~400 ka (Waelbroeck et al., 2002) are proposed for the marine terraces.

Two ages from terraces T2 and T3 (samples 1b and 5, Table 2) on the Pollino border were consistent with an attribution to the MIS 5.3 and MIS 5.5, respectively, but the samples were ostensibly resedimented in the underlying terraces. From this same area Cucci (2004) obtained a ~130 ka age from our T4 terrace (sample 6a, Table 2). An age of 135 ± 20 ka, consistent with an attribution to the MIS 5.5, was obtained for sample 3a coming from T4 on the Sila border, although an older age consistent with attribution to MIS 7 was obtained at the same site for sample 3b. Finally, a ~43 ka ^{14}C calibrated age on a shell coming from T1, but ostensibly resedimented, provided nevertheless the existence of the MIS 3.3 (sample 4, Table 2).

However important those limitations may be, the accurate attribution of a terrace to a particular highstand do not compromise our analysis of the recent deformation field. Of particular relevance here is the attribution of T4 to the MIS 5.5, a prominent marker for deformation (Bordoni and Valensise, 1998; Ferranti et al., 2006). Our radiometric result for T4 is consistent with the observation that this is the widest terrace in the region, as typically observed elsewhere in the central Mediterranean Sea (Ferranti et al., 2006). The resulting average uplift rate, as established by previous works (Westaway, 1993; Cucci and Cinti, 1998; Cucci, 2004), approaches ~1 mm/yr. The identification of intermediate terraces (e. g. MIS 3) presented here and fully discussed in Santoro et al. (2009) suggests that uplift was not linear, but partitioned in periods of higher and lower rate.

3.2. Geomorphic indices of active deformation

3.2.1. Methods

In order to retrieve information on the active three-dimensional displacement field in the region, the study of deformed marine terraces was supplemented with an analysis of fluvial anomalies (Fig. 6). We calculated over the main drainage basins those indices (Fig. 7) of the relative youthfulness of the landscape suggestive of active tectonics. The indices values are shown in Fig. 7 along a compound topographic profile (Fig. 7a) traced roughly parallel to the marine terraces deformation profile from Pollino to Sila ranges, allowing comparison between coastal and fluvial markers of deformation.

The SL (stream length-gradient) index (Fig. 7b) quantifies the departure of the stream longitudinal profile from the concave equilibrium shape typical of a graded stream. The SL index has been calculated over discrete parts of tributaries (higher order streams, where, unlike with the major rivers, sedimentary processes may have not yet reset the tectonic signature), using the reading:

$$SL = (\Delta H / \Delta L) * L,$$

where $\Delta H / \Delta L$ is the stream slope with ΔH the difference in elevation and ΔL the length of the analyzed stream tract, and L is the stream length from the head to the tract midpoint. Index anomalies (higher SL

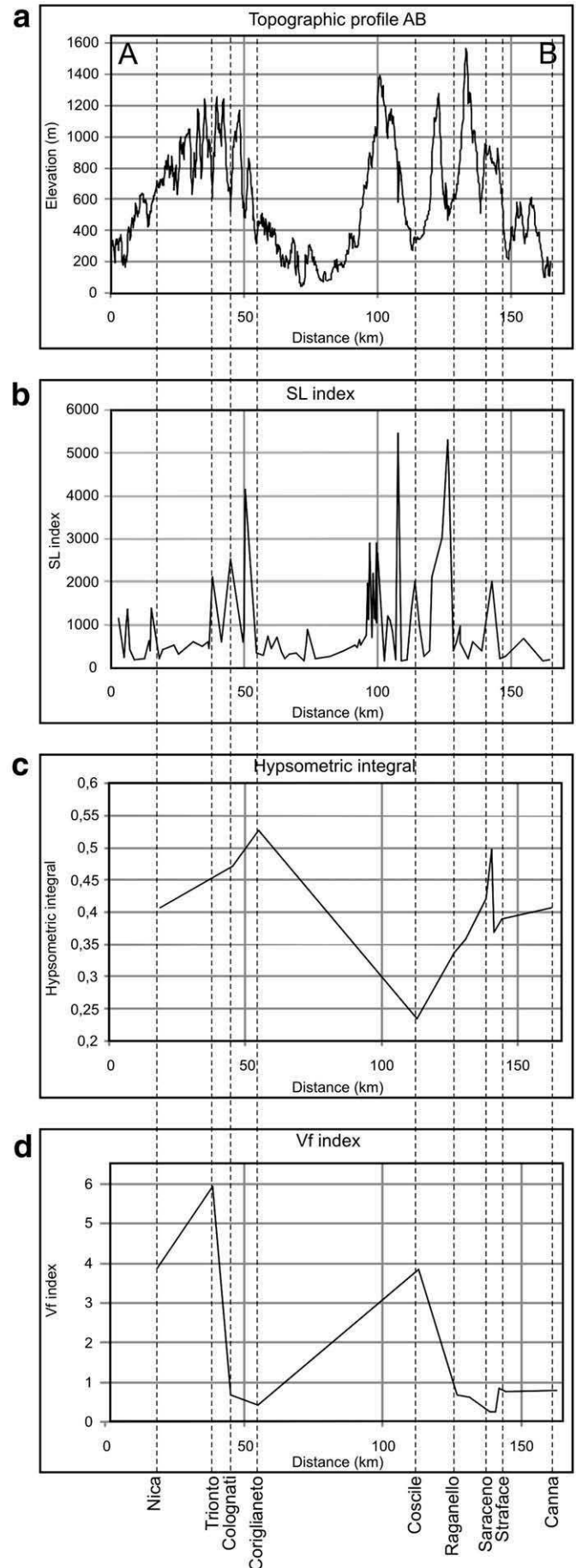


Fig. 7. Geomorphic indices computed along a compound profile parallel to the coastline (see Fig. 6 for location). (a) Topographic profile. (b) SL index. (c) Hypsometric integral. (d) Vf index.

values) may identify areas where, unless a dominant lithological control is proved, focused active deformation can be inferred. The SL index was computed over several hydrographic networks extracted from a publicly available (<http://88.41.139.89/cartografia/>) 40×40 DEM built from 1:10,000 scale maps. A total of 428 streams subdivided in 8870 tracts were analyzed adopting a spatially uniform sampling rate of 3 points/km² in order to avoid interpolation errors. A contour map of the SL index was constructed through a gridded Kriging interpolation using 1×1 km cells, with the index values attributed to the cell nodes (Fig. 6).

Other parameters extracted from the cartographic database are the Hypsometric integral and Vf index. The Hypsometric integral (Fig. 7c), which is the area below the hypsometric curve, is a qualitative measure of how fast a drainage network reacts to external

tectonic perturbations, with high values signaling active uplift. The Vf index (ratio of valley floor width to valley height, Fig. 7d) helps to identify narrow and incised valleys, with low Vf values, that are suggestive of active uplift, and is given by:

$$Vf = 2Vfw / [(Eld - Esc) + (Erd - Esc)],$$

where Vfw is the width of the valley floor, Eld and Erd are elevations of the valley divides and Esc is the elevation of the valley floor.

3.2.2. Results

Fluvial anomalies show a conflicting pattern moving parallel to the coastline from the high and dissected Pollino range to the low-lying Sibari plain and up again to the plateau-shaped Sila range (Fig. 7a).

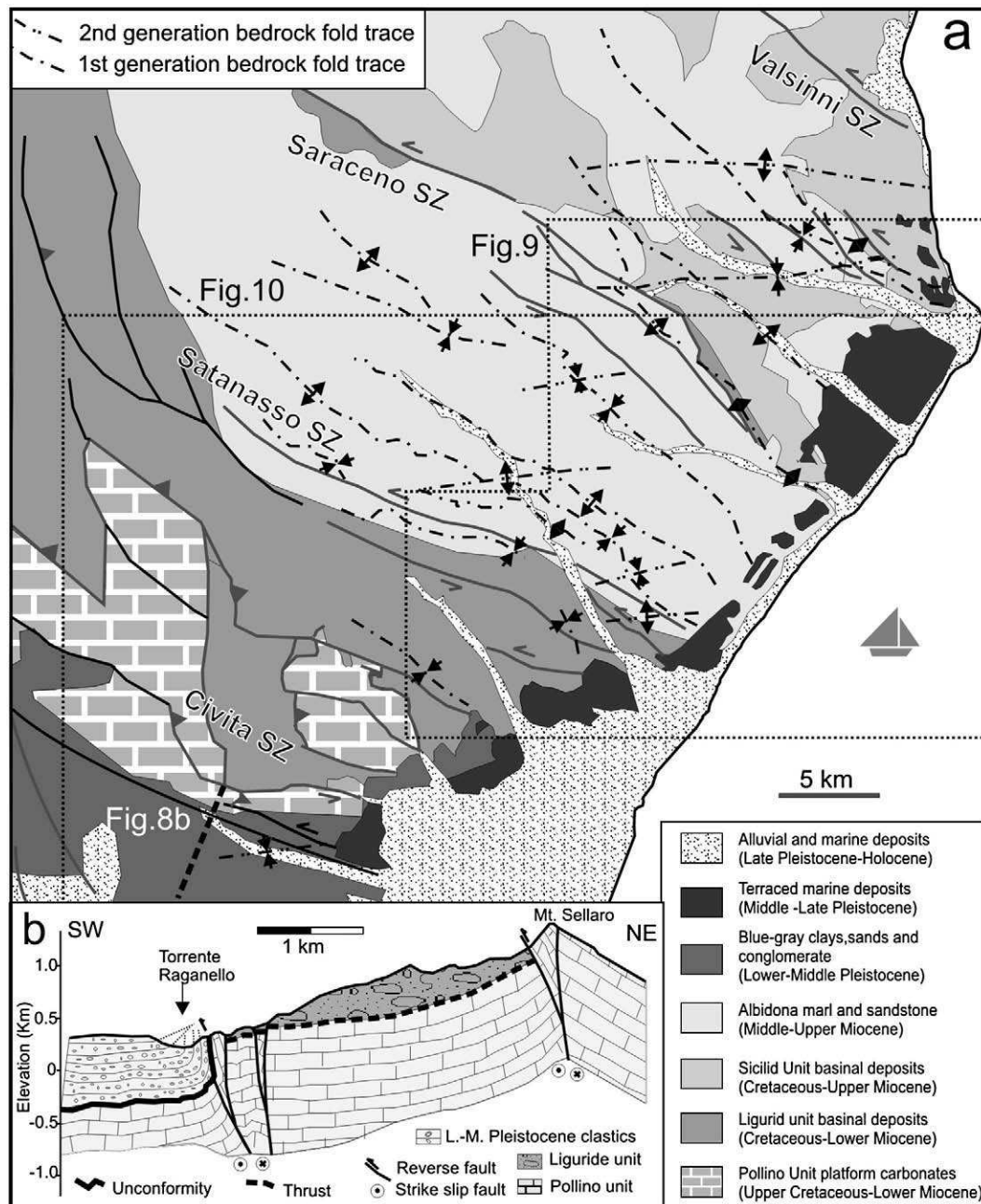


Fig. 8. (a) Generalized structural map of the Pollino range coastline showing the relation between two fold generation axial traces (partly based on Cesarano et al., 2002). (b) Geological profile on the southern border of the eastern Pollino range, showing SW-directed folding of Pleistocene deposits related to growth of the Pollino fault-related anticline (modified after Hippolyte et al., 1992, and Monaco et al. 1998).

Specifically, high values of the SL index (Fig. 7b) and hypsometric integral (Fig. 7c) and low values of the Vf index (Fig. 7d), are recorded for the Pollino sector between the Coscile and Canna streams, at the same location where the marine terraces attain a high regional elevation (Fig. 5).

By contrast, relatively low values of the SL index and hypsometric integral, and high Vf index values are found in the central stretch between the Coscile and Coriglianeto streams, (Fig. 7b–d). This pattern spatially coincides with the subdued topography of the Sibari plain (Fig. 7a), where regional elevation of marine terraces keeps relatively minor (Fig. 5). Where this elevation increases in the Sila range, in particular at the border of the plateau between the Coriglianeto and Trionto stream, the SL index and hypsometric integral are high again, and the Vf index is low (Fig. 7a–d).

These observations suggest first-hand distinction of morphotectonic domains, with actively rising mountain ranges and less rapidly uplifting plain. Given the fact that such regional patterns hold within individual domains irrespective of lithological boundaries existing within those domains (Fig. 6), a lithological control on these patterns, although certainly existing, is probably subordinate relative to tectonic processes.

Unlike the Hypsometric integral and Vf index, which only provide smoothed regional patterns, the SL index is suited to identify spatial differences attributable to local deformation processes within more focused segments (Figs. 6 and 7b). In the north, several NW-SE trending anomalies (with SL index >550) stretch across lithological boundaries and stream courses (Fig. 6), and possibly reflect the trend of actively growing ridges. In the Sila massif, the anomaly pattern is more complex and it may be controlled at some degree by stream orientation.

3.3. Structural fabrics

We present in this section an analysis of the structural frame of the south-eastern side of the Pollino range east of the well investigated Pollino–Castrovillari normal fault, which is part of the active fault belt dissecting the western side of southern Italy (Fig. 3). The aim of this analysis is to provide evidence that, within this region, the last generation of structural fabrics (folds and transpressional faults) detected in the bedrock and involving Lower to Middle Pleistocene deposits has a marked spatial coincidence with the major terrace disturbances and geomorphic anomalies, suggesting the continuation of the transpressive displacement field into the Late Pleistocene. Our field work was focused on fold fabrics orientation and fault slip lineation analysis, supplemented with results drawn from existing publications (Appendixes A and B). Fault data were analyzed by means of the inversion technique of Marrett and Almendinger (1990) in order to find the orientation of the principal kinematic axes related to a particular fault set. At least three, but usually more than five non-parallel striated faults where used for determination of the displacement axes at any specific locality (see Appendixes A and B).

Our analysis revealed the existence of both transpressional and extensional fabrics, which are segregated within distinct spatial compartments and at different structural levels. Whereas transpressional structures in bedrock and cover are distributed within the mountain range and at its borders, the normal faults are basically retrieved in the Lower Pleistocene clay and overlying terrace deposits outcropping on the range-fringing coastal plain (Figs. 8a–10).

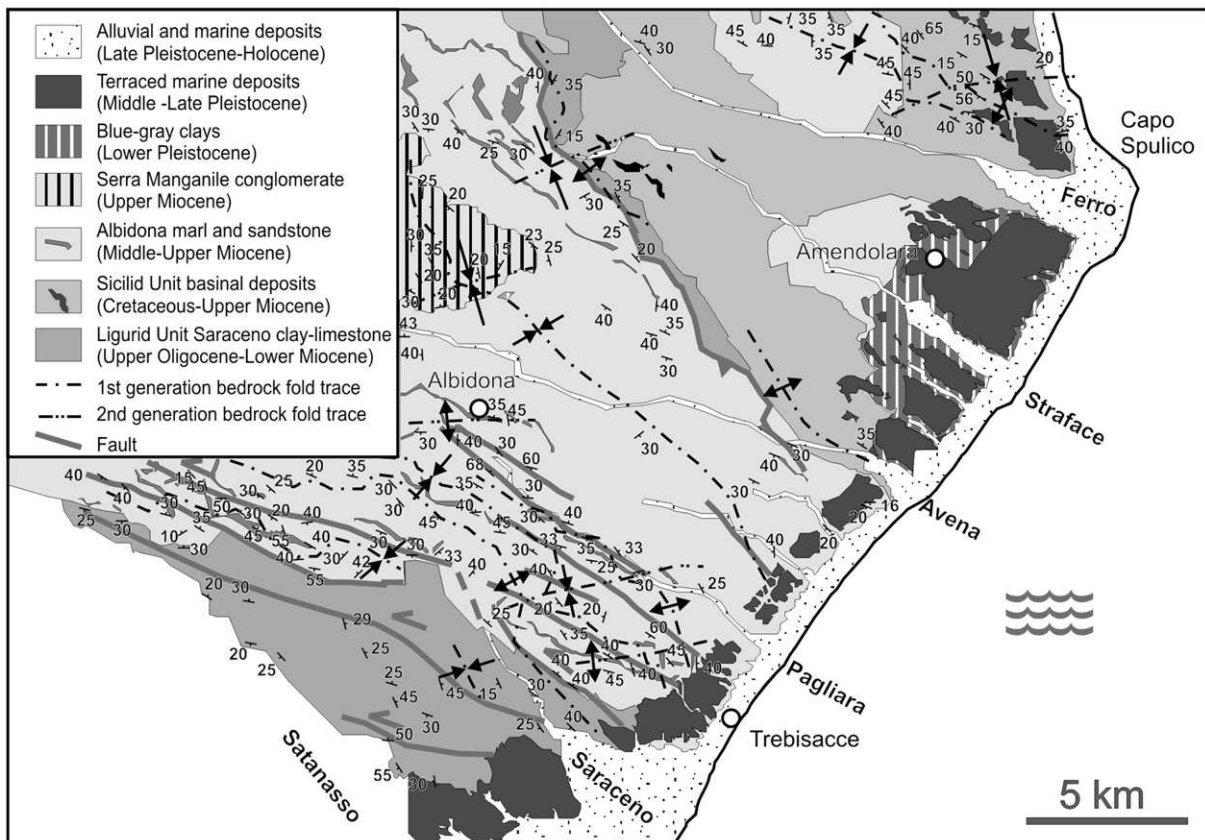


Fig. 9. Structural map of the area between Trebisacce village and Capo Spulico (location in Fig. 8a), showing the relation between two fold generation traces as constrained by bedding dispersal.

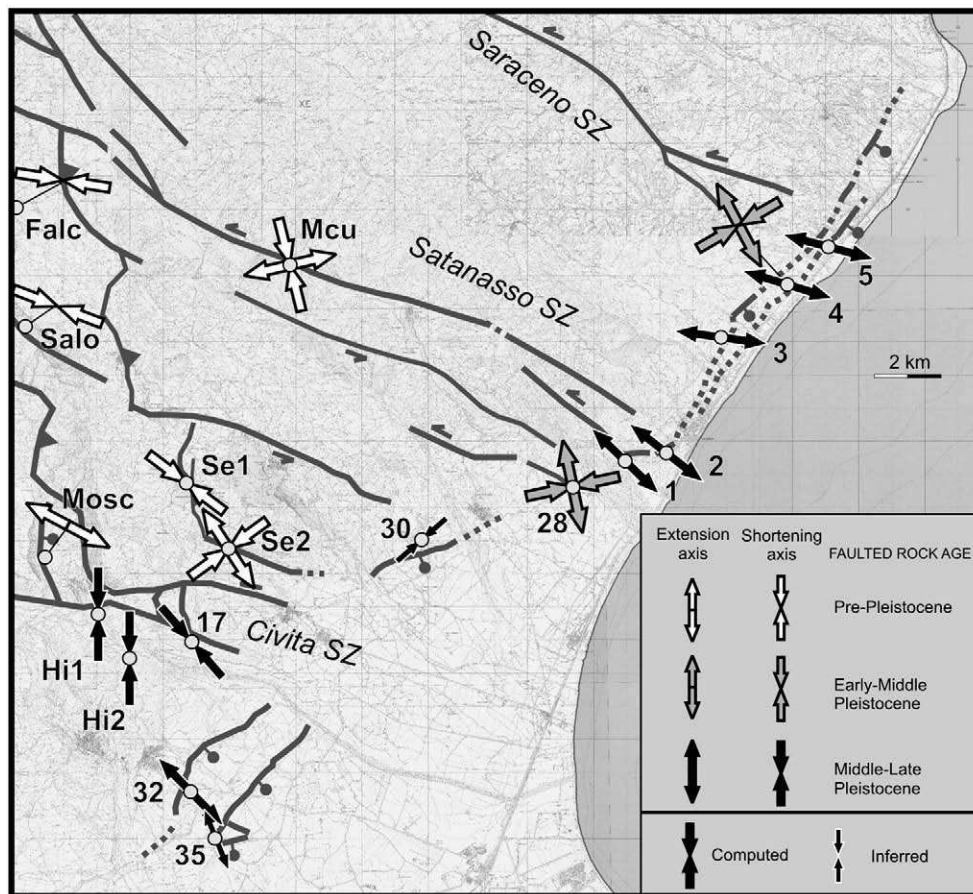


Fig. 10. Kinematic map of the southeastern Pollino range, showing the horizontal trend of the finite deformation axes (contractional, extensional, or strike-slip regime) based on inversion of fault-slip lineations measured at sites shown in the map. Site fault slip diagrams are shown in Appendixes A and B.

3.3.1. Folds and transpressional faults

Two generations of folds with differently oriented axes are mapped within pre-Quaternary rocks of the Pollino range, and are best traced within the Ligurid and Sicilid basin deposits and overlaying Albidona marl and sandstone (Figs. 8a and 9). The first generation involves two systems of NW-SE striking, recumbent to upright, serrated folds within the Albidona deposits, with the second structures refolding the previously enucleated fabrics (e. g. Cesarano et al., 2002). This pristine fold generation broadly follows the major tectonic contacts between the different litho-tectonic assemblages, and ostensibly forms the dominant pattern in the area (Fig. 8a), as elsewhere in the Apennines.

Superposed on these folds, a second generation of ~E- to ENE-striking, upright and gentle folds is observed, forming a weak dome-and-basin interference structure (Fig. 8a). The younger fold system can be traced by means of map-scale analysis and has gently deformed the previous orogenic fabrics, as indicated by bending of older tectonic contacts and by dispersal of previously folded beds (Fig. 9). Cesarano et al. (2002) limited their analysis to pre-Pliocene rocks, and dated the second fold generation to the post-Early Pliocene.

Our analysis not only confirms the development of the younger fold set in the Mesozoic–Cenozoic basinal rocks, but also documents that it can be traced in Pleistocene deposits. Along the southern border of the Pollino range, Lower–Middle Pleistocene fan sediments (Vezzani, 1968) form a km-scale, southerly-asymmetric syncline. Fold growth during deposition is shown by bedding attitudes, with strata that are straight to locally overturned at the mountain front, and progressively less deformed away from it (Fig. 8b). Sediments involved in folding

developed meso-scale reverse and strike-slip faults which were tilted together with bedding during ~N–S shortening (sites Hi1 and Hi2, Fig. 10; Hippolyte et al., 1992). Nannoplankton analysis performed by Hippolyte et al. (1992) indicates that part of the tilted sedimentary section is less than 460 ka old. Progressively younger fan generations have southward shifting depoaxes and truncate tilted strata, indicating deposition during uplift of the mountain front (Fig. 11a).

Further away from the mountain front, fan deposits laterally correlative of marine terrace T6, that we attribute to MIS 7.3 (~215 ka, Table 1), are tilted and affected by reverse shear bands (Fig. 11a and b). These bands are marked by a cm-scale sandy gouge (Fig. 11c), and clast-striation analysis suggests NW-SE oriented shortening (site 17; Fig. 10).

Brittle transpressional fabrics is represented by high-angle ~WNW-ESE striking, right-hand en echelon left-oblique faults which are arranged in distributed fault arrays (Fig. 8a). Thrusts and reverse faults with ~N–S strikes and westerly sense of transport branches out from the strike-slip faults (Fig. 8a). Along the Civita and Saraceno fault arrays, on both sides of the Pollino range, Lower–Middle Pleistocene conglomerates are reportedly involved in transpressional faulting (Monaco, 1993). Fault slip lineation analysis in pre-Pleistocene rocks along the Civita shear zone indicates that slip was partitioned on the left oblique and thrust faults, which record ENE–WSW and ESE–WNW shortening directions, respectively (sites Se1 and Se2; Fig. 10). To the east, at the southeastern tip of the Satanasso and Saraceno shear zones, the Early Pleistocene clays are affected by left-oblique faults active during NE–SW shortening (sites 28 and 4, Fig. 10), a pattern resembling that found on bedrock faults of the

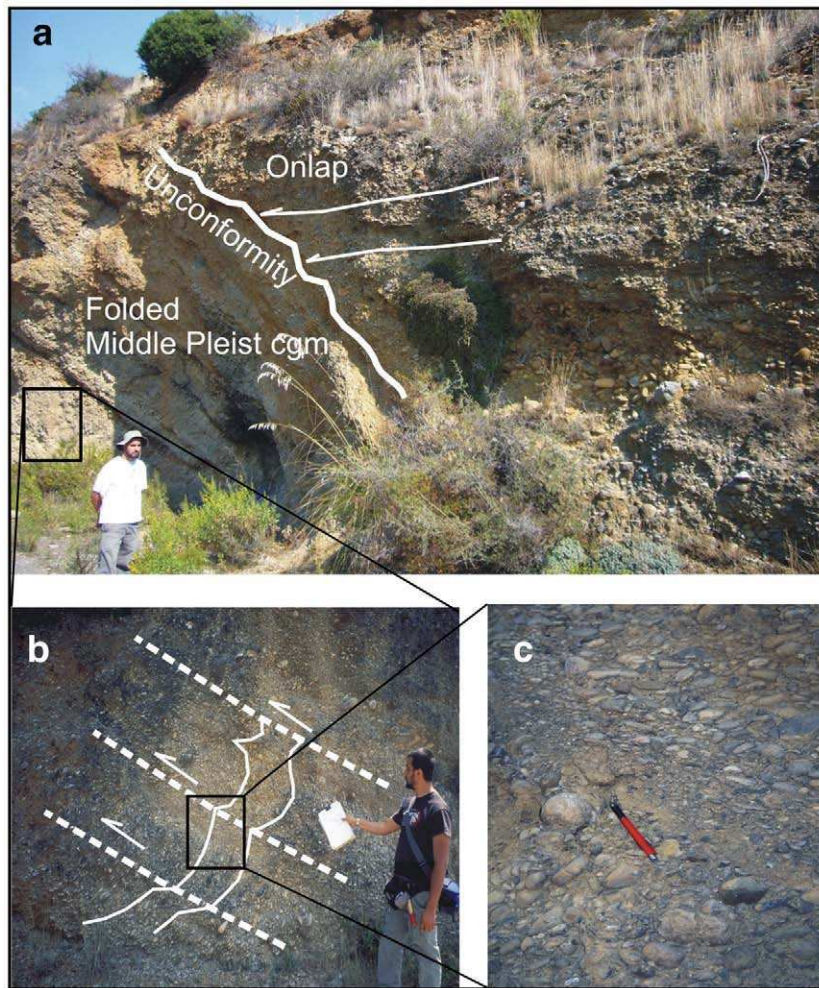


Fig. 11. (a) Folded Middle Pleistocene fluvial conglomerates along the Raganello stream on the southern border of Pollino range (location in Fig. 4). (b) Detail of shear bands within the conglomerate. (c) Close-up of a shear band.

Civita shear zone. South of this site, Middle Pleistocene sands and conglomerates are tilted and cut by meters-scale reverse faults indicating NE–SW shortening (site 30). The tilted rocks and faults at this site are sealed by marine deposits correlative to T6 and aged to 215 ka (Table 1).

In summary, a complex 3-D pattern of shortening and transpression is recorded in the eastern Pollino range. Although the major shear zones acted as left-oblique during an ~NE–SW trending shortening (see also Monaco, 1993) a broad ~N-trending shortening is recorded at the range southern border. Here, the mountain front east of the Pollino–Castrovillari fault is not normal fault-controlled. Rather, it represents the steeper limb of a southward asymmetric range-scale fold enucleated in the platform carbonates and involving up to ~215–450 ka old sediments (Fig. 8b). Finally, the coastal side of the range experienced transpression with ~ENE-trending shortening axis after the Early Pleistocene.

3.3.2. Extensional faults

Dip-slip to slightly oblique extensional faults of the Avena–Lauropoli system have been mapped on the northern side of the Sibari plain, where they cut through terraces as young as T2 (Figs. 4, 5, and 12). Evidence of faulting has been found in a northern and a southern sector, separated by an intervening 10 km stretch where no fault was observed (Fig. 10). The southern strand of the fault does not appear to stretch westward beyond the Coscile stream (Fig. 4). Thus, as

for the transpressional fabrics, slip on the Avena–Lauropoli fault appears confined east of the active Pollino–Castrovillari normal fault (Fig. 3).

Within the northern sector, which stretches between the Sata-nasso and Ferro streams, the fault is expressed by a series of short scarps, locally disposed in stair-step fashion (Figs. 5 and 10). The summed vertical offset stipulated by means of stratigraphic and morphologic offset of terrace T3 (Fig. 12c), is up to 15–20 m (Fig. 5). Within the southern segment stretching between the Raganello and Coscile streams (Fig. 11), the vertical offset as estimated by the projected position of terrace T5 is up to 50 m (Fig. 5). When the offset is estimated on the predicted position of terrace T4, it is ~30 m (Fig. 5). Given the inferred terraces age (Table 1), all these estimates are consistent with a 0.2–0.25 mm/a vertical slip rate.

Outcropping fault surfaces have either a low- (~30°) or a high- (~50°–60°) angle of dip (Fig. 12a and b, respectively). Low-angle faults are marked by a prominent tilting of beds into the fault plane (Fig. 12a). Kinematic analysis of slip lineations preserved on striated fault surfaces indicates a predominant extensional displacement (Fig. 10). The computed extensional axis trends ~NW–SE, orthogonal to the coastline and to the topography (Fig. 10).

In summary, extension down to the Ionian Sea does not occur along a through-going fault system, but rather involves separate scarps with different detachment levels as indicated by the abrupt lateral variation in hanging-wall tilts. Of significance, a spatial

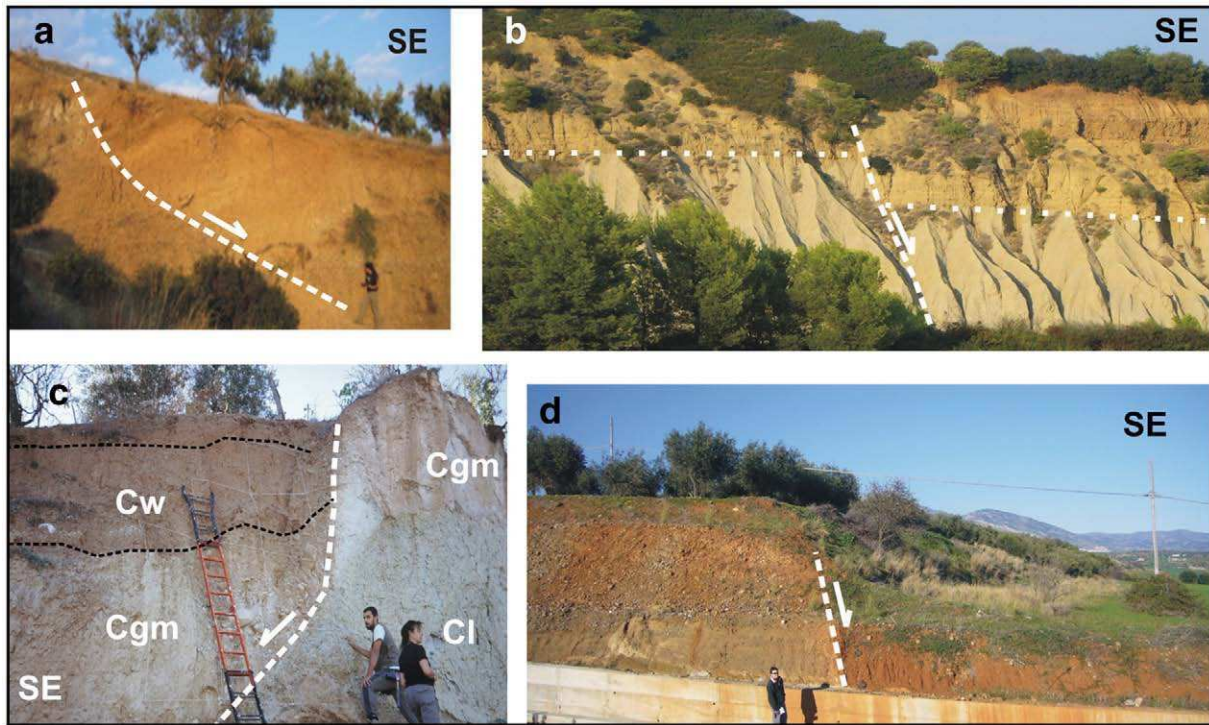


Fig. 12. Outcrops of the Avena–Lauropoli fault. (a) Outcrop south of the Avena stream (location in Fig. 10). Note marked tilting along listric shear plane. (b) Outcrop at the Avena stream showing the dip-slip displacement of terrace T3 and of its basal unconformity indicated by a dotted line (location in Fig. 10). (c) Outcrop at Trebisacce village. The fault cuts through the Lower Pleistocene clay bedrock (cl) and overlying marine sands and conglomerate (cgm) of T3, creating a colluvial wedge of continental deposits (cw) in the hanging-wall (location in Fig. 10). (d) Outcrop at Lauropoli village, with the fault cutting through T5 deposits (location in Fig. 4).

separation emerges between the mountain belt undergoing transpression and shortening, and the coastal strip where the more surficial deposits record extension (Fig. 10).

3.4. Offshore structural architecture

Fundamental constraints on the structures mapped or inferred on-land can be placed through the analysis of publicly available (<http://www.socgeol.info/pozzi/index.asp>) multichannel seismic reflection profiles supplemented by oil-exploration well logs (Fig. 13a). Chronostratigraphic and seismic data offers excellent markers that can be laterally traced along the profiles. The best developed reflector is the unconformity which truncates the Messinian (Late Miocene) evaporitic and clastic rocks and forms the base of an unevenly thick Pliocene–Quaternary depositional package (Fig. 13b and c). Locally, the abrupt transition between the Lower Pleistocene clay and the overlying Middle–Upper Pleistocene coarser clastic sequence forms an identifiable reflector which can be used to decipher the more recent structural evolution.

Analysis of a dense grid of seismic profiles (inset in Fig. 13a) illustrates that the structural pattern of the SW sector of the Taranto Gulf is dominated by thrusts and transpressional faults that bound structural highs and lows (Fig. 13a). The frontal ridge is limited eastward by the markedly curvilinear front of the thin-skinned thrust belt, and is bound to the NE by the low-lying foredeep basin. A satellite basin (Sinni basin) separates the frontal ridge from the more internal and elevated Amendolara ridge (Fig. 13a and b). The structural thickness of the thin-skinned thrust belt increases to the SW from ~2.5 sec TWT beneath the frontal high to in excess of 5 sec TWT beneath the Amendolara ridge, and is mostly composed of imbricated Miocene and younger deposits (Fig. 13b). The Apulian carbonate platform, found at the sea-bottom to the NE, plunges southward underneath the foredeep basin and the thrust belt, and is itself involved in thrusting.

Cross-cutting relations suggests that early shortening was accommodated by gently-dipping, NE-displacing thrusts which repeatedly imbricated the Miocene deposits and, in more internal sectors beneath the Sila coastline, the Calabrid and the deeper Apenninic thrust sheets (Fig. 13b). These thrusts are cut by steeper reverse and transpressional faults which mostly displace to the SW and represent back-thrusts in the regional reference frame (Fig. 13b). The backthrusts emanate from underneath the Apulian platform and, at more surficial levels, they branches with several splays within the Messinian evaporite, which provides a preferred detachment level. The younger faults clearly truncate the unconformity between the Lower Pleistocene clay and younger deposits, and tilting and depoaxial shifts within the Upper Quaternary package supply further evidence of the recent activity of some faults (Fig. 13b and c). Line-balancing techniques indicate that the backthrusts control the present ridge-and-basin morphobathymetric arrangement. Significant back-thrusting has been accommodated on the southern side of the Amendolara ridge, where it controlled the development of a deep (~3 sec TWT) through in the Sibari basin, filled by Upper Pliocene–Quaternary deposits (Fig. 13b). A large fraction of the ~1.8 sec TWT vertical offset accommodated along the deformation belt, here named Amendolara backthrust fault zone (ABFZ), was accrued during the Middle–Late Pleistocene as suggested by growth relations on the southern side of the ridge (Fig. 13b). A more internal high (Luana High) is found SW of the Sibari basin, and its NW–SE trend is indicated by alignment of oil drills (Fig. 13a and b).

In detail, the faults bounding highs and lows have curvilinear traces akin to the pattern which characterizes the fault systems found on-land in the Pollino and Sila ranges (Fig. 13a). The ABFZ swings from NW–SE in the east to ~N–S north of Cape Trionto, and then ~E–W approaching the coastline (Fig. 13a). On the westward sector of the ABFZ close to the coastline, a major backthrust active during the Middle–Upper Pleistocene bound the SW side of the Larissa high

(Fig. 13c) and can be straightly traced to join the Satanasso shear zone to the west (Fig. 13a). To the south, the backthrusts bounding the Luana High (Fig. 13b and c) can be merged on-land with the Civita shear zone along the southern side of the Pollino range. Other transpressional systems found offshore north of the Amendolara ridge can be laterally correlated with the Saraceno and Valsinni shear zones (Fig. 13a).

Finally, slumping or creeping at more surficial levels occurs above listric normal faults localized on the steeper flanks of the Amendolara and frontal ridges (Fig. 13b). Marker correlation suggests that the listric faults are rooted within the Lower Pleistocene clays at depths no higher than those equivalent to 1.5 sec TWT (Fig. 13b). These situations

are similar to the tilted structural panels found on-land along the Avena–Lauropoli fault (Fig. 11).

3.5. Seismicity analysis

Although northern Calabria was devastated by large historical earthquakes (e. g. Galli and Bosi, 2003), the region has not been struck by significant seismic events during the instrumental era. Notwithstanding, recent low to moderate magnitude crustal events can be used to highlight the contemporary deformation pattern. For this analysis, we rely (Table 3) on a set of 2005–2007 focal mechanisms ($3.0 \leq M_l \leq 4.0$) calculated by Mucciarelli (2007), supplemented by

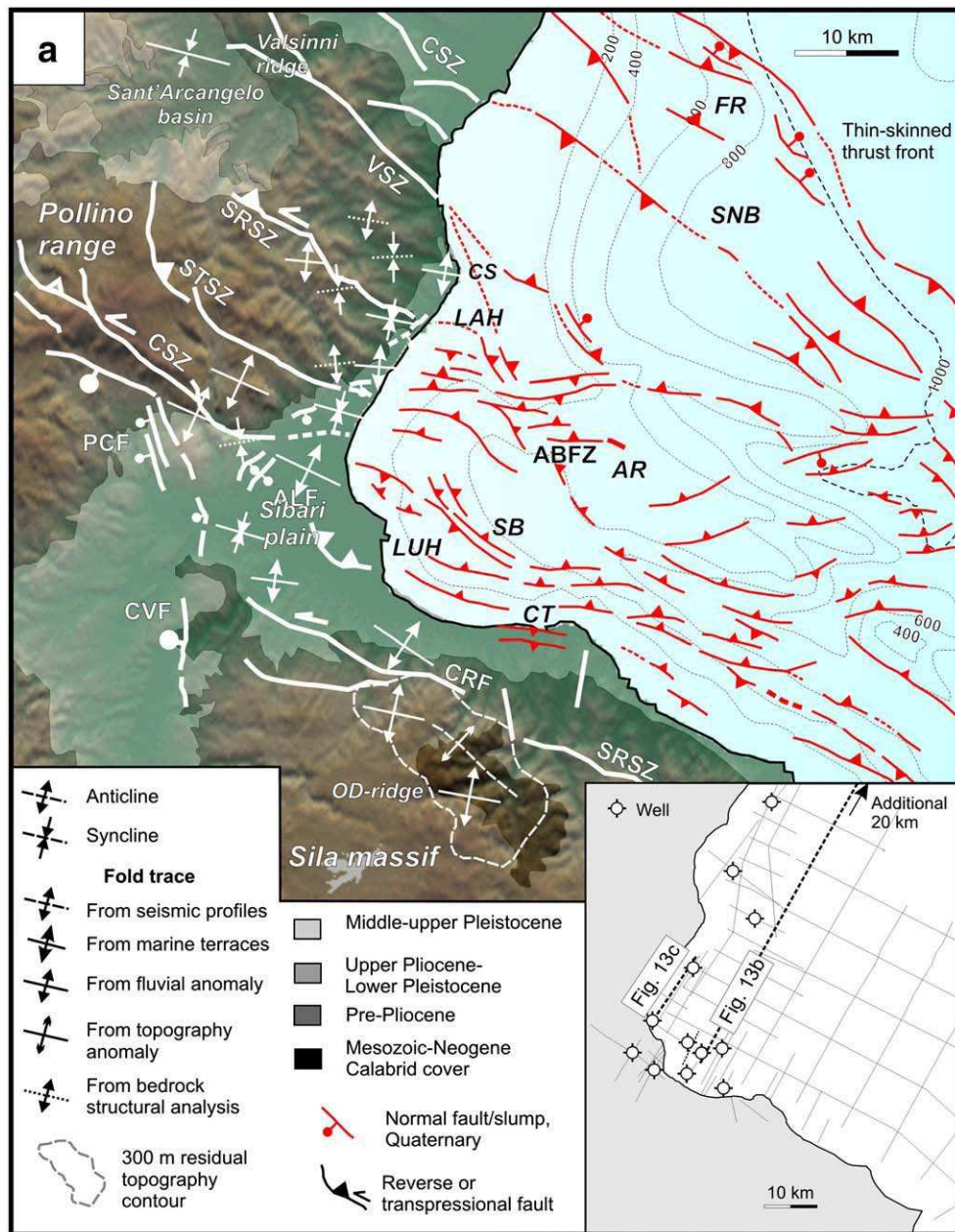


Fig. 13. (a) Structural map of northeastern Calabria showing the main Pliocene–Quaternary structures mapped on-land and imaged offshore. The grid of seismic profiles used for constructing the structural map offshore and along the coast is shown in the inset. Faults labeled as in Fig. 3. Location and trend of topography anomaly in northern Sila from Molin et al. (2004). (b). Seismic reflection profile F75–89, top, and its line-drawing, bottom (location in a). L = Lower; M = Middle U. = Upper. (c) Seismic reflection profile DF80–35, top, and its line-drawing, bottom (location in a). L = Lower; M = Middle U. = Upper.

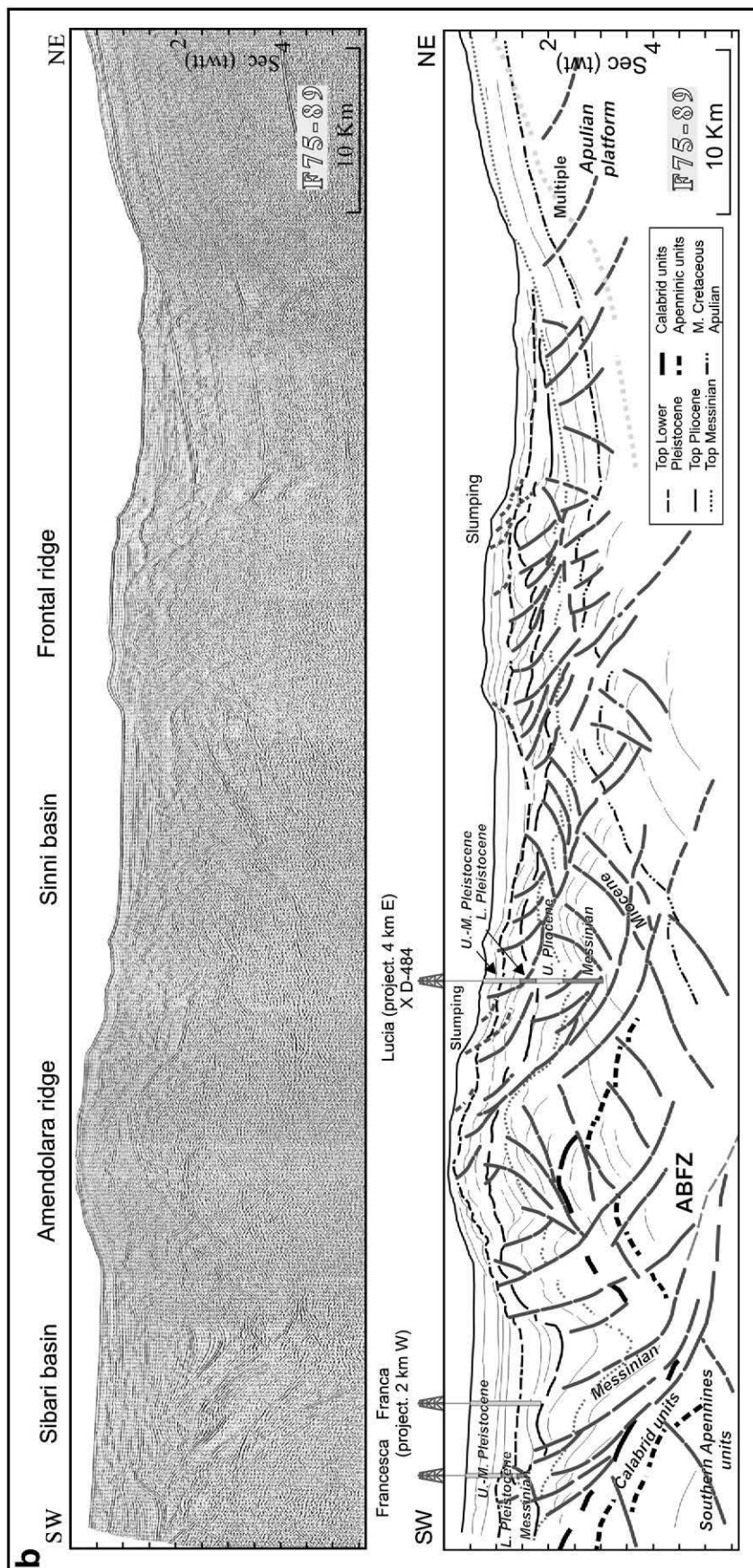


Fig. 13b (continued).

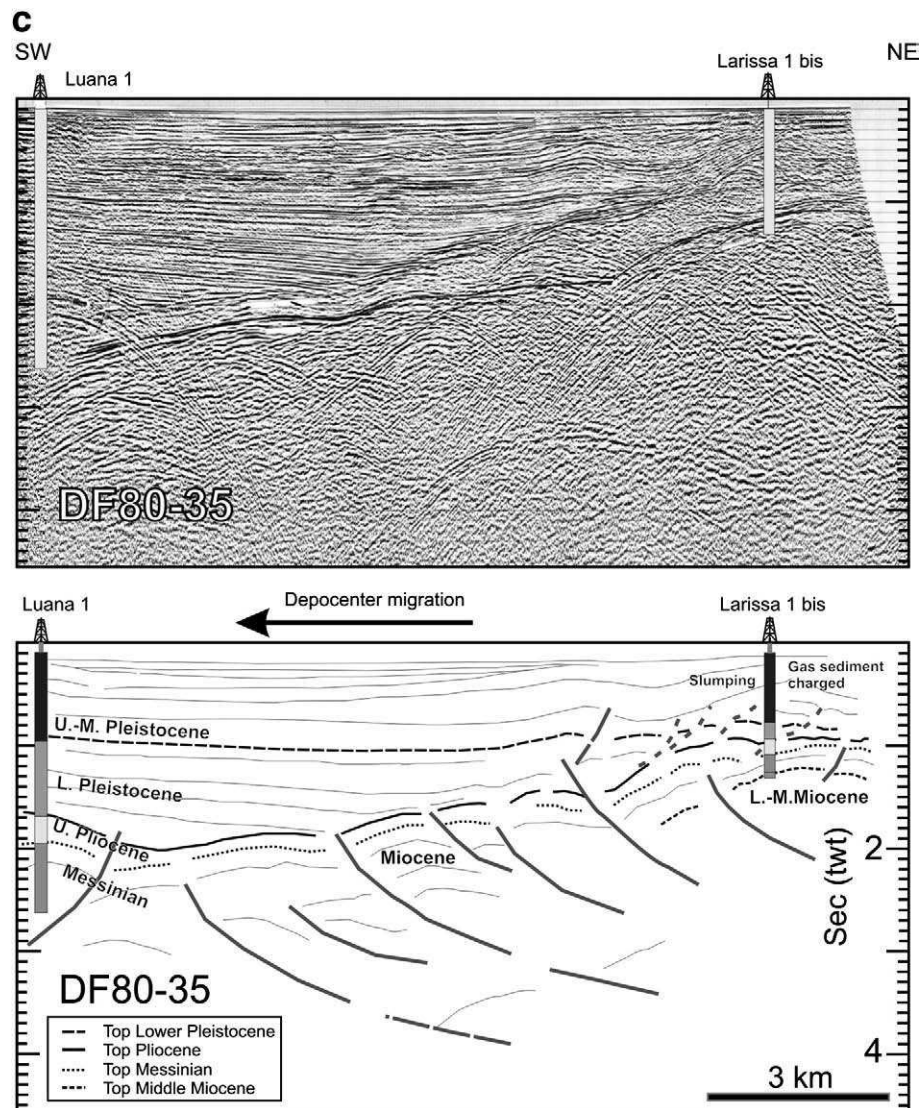


Fig. 13 (continued).

Regional CMT fault-plane solutions ($4.0 \leq M \leq 4.7$) retrieved from the Mednet catalogue, and by first-arrivals ($3.2 \leq M \leq 3.9$) fault-plane solutions from Frepoli and Amato (2000).

Although at a first glance the kinematic pattern appears complex, when focal mechanisms are viewed in relation to the reconstructed structural frame, some systematic relations emerge (Fig. 14). The most energetic shocks concentrate along the coast of Sila and in the near offshore. Seaward of the Sibari plain, a mixture of thrust and strike-slip earthquakes are aligned with the ABFZ along the southern flank of the Amendolara ridge (Fig. 14). A second belt of thrust and strike-slip focal solutions is found to the south at the NE flank of the Sila massif and spatially coincides with the trace of the Corigliano–Rossano and S. Nicola–Rossano faults (Fig. 14). Both at the northern and southern seismic belts, the NW–SE nodal planes parallel the trend of bedrock structures, and are consistent with marine geophysical and on-land structural data. The P axis of the incremental strain tensor trends almost consistently ~ENE–WSW for both thrust and strike-slip earthquakes, and indicates substantial thrusting and left-transpression on the NW–SE striking structures (Fig. 14). Few extensional earthquakes with NE–SW nodal planes are located between the two transpressional belts at the latitude of Capo Trionto (Fig. 14). At the

surface, extensional faults with broadly similar trend are mapped on land (Randisi, 2007), and probably represent a local negative bend. Note that three out of four extensional mechanisms are from the relatively old work of Frepoli and Amato (2000), based on a coarser, regional network distribution, and thus errors on localization and kinematics may be substantial.

Most of the events are located within the sedimentary upper crust above ~15–25 km depth (Fig. 14 and Table 3). This depth is roughly set at the base of the underthrust Apulian foreland platform, which has a ~6 km thickness (Catalano et al., 2001), and dips to the SW under the accretionary prism whose thickness increases from NE to SW from ~10 km beneath the Amendolara ridge (Fig. 13b) to ~20 km beneath the Sila range (Cello et al., 1982; Van Dijk et al., 2000). The extensional earthquakes are located within the accretionary wedge at depths of ≤ 10 km. An extensional earthquake beneath the Sinni basin was at very shallow depth (n. 1, Fig. 14), consistent with the listric normal faults rooting at shallow levels in seismic reflection profiles (Fig. 13b). The largest thrust and strike-slip events, instead, are recorded beneath ~15–25 km depth within the Apulian sedimentary crust and crystalline basement (Fig. 14). Few thrust and strike-slip events at the border of Sila massif are located at 7–15 km depth at the

base of the accretionary prism. A pure thrust event (n. 13, Fig. 14) is located at ~7 km beneath the Luana High in the innermost part of the Sibari basin and possibly occurred on one of the backthrusts imaged on the SW side of section F75–89 (Fig. 13b).

Epicenters from the ASSN (1966–2003) and INGV (1981–2002) catalogues, and from a local seismic network, roughly outline the trace of major bedrock structures. Although the largest number of epicenters ostensibly coincides with the trace of known active normal faults in the west, two epicenter belts illuminate the NW–SE-trending transpressional fronts at the Amendolara ridge and north Sila massif (Fig. 14).

4. Discussion

4.1. Origin of local deformation of marine terraces and fluvial geomorphic anomalies

The deformation profile of marine terraces along the Ionian Sea coast of northern Calabria reveals that uplift embeds two deformation components. As already pointed out in previous studies (e. g. Westaway, 1993; Cucci and Cinti, 1998; Ferranti et al., 2006), the largest contribution to uplift is provided by a regional component that slopes gently to the NE across the Apennines (Fig. 2). Obviously, the gradient in deformation is notable at a spatial scale larger than the study area, where regional uplift rate attains a plateau at ~1.00–1.25 mm/a (Fig. 2).

Superimposed on this, a smaller wavelength, differential uplift, whose amplitude increases with the terrace age, can be appreciated in the study area. Moving southward from Capo Spulico, the terrace inner margins form a northern culmination with secondary bumps (Fig. 5), a pattern which continues to the north toward the Bradano foredeep (e. g. Cucci and Cinti, 1998). The major differential uplift is observed in a narrow corridor centered between the Saraceno and Avena streams, with a maximum rise of ~20–30 m for terraces from T2 to T6 (Fig. 5). South of this location, the terrace elevation drops of few tens of meters between the Saraceno and Satanasso streams (Fig. 5). A second, major high is centered between the Coscile and Satanasso streams (Fig. 5). By contrast, a dramatic down-warping in the whole terrace flight elevation is observed further south between the Coscile and Crati streams. South of this site, the ~10–20 m amplitude waveforms are developed over a background plateau (Fig. 5). Several minor amplitude undulations can be traced on these local highs and lows in the marine terrace elevation profile.

Given uncertainties, our analysis indicates local contribution to uplift of up to ~30 m for a terrace uplifted at ~95–130 m elevation (T4, with a 124 ka age). Thus, the regional vs. local uplift ratio can be roughly estimated at ~3:1 to ~4:1. For this analysis, we pinpoint on the regional elevation of the terraces at the northern limit of the study area (e. g. 115 m for terrace T4). We are aware, however, that the regional deformation also incorporates local components of uplift summed from north of this site.

The small wavelength component in the deformation profile of marine terraces in the area was attributed by previous workers (Cucci and Cinti, 1998; Cucci, 2004) to local sources, namely to footwall uplift along the Pollino–Castrovillari normal fault, and, further north, to a yet poorly characterized fault which was observed at the Avena stream mouth (Fig. 4). Although the proposed interpretations is feasible, the arguments discussed hereinafter suggest an alternative view.

Firstly, we note that the local deformation is not solely restricted to the area where slip on the Pollino–Castrovillari fault (and possibly the Avena–Lauropoli fault) would cause permanent strain. Rather, the undulations in the uplift profile are distributed pervasively across the whole coastline (Fig. 5). In addition, in order to be related to the extensional displacement field controlling slip on the Pollino–

Castrovillari fault, the km-scale undulations mapped within the whole terrace flight would require as many spaced extensional faults at a high-angle to the coastline, which have not been observed. Neither the evidenced normal slip on the Avena–Lauropoli fault, which is broadly orthogonal to the coastline (Fig. 10), can justify the undulations observed in the reconstructed paleo-shorelines. Finally, although a contribution from the Pollino–Castrovillari fault could be embedded in the deformation profile, this fault is located too far from the raised shorelines (Figs. 3 and 4) to cause significant footwall uplift according to elastic dislocation models (e. g. King et al., 1988).

Based on our integrated geomorphologic and tectonic analysis, we argue that the local anomalies are best concealed with regularly distributed anticline–syncline fold trains. This interpretation is consistent with the overall tectonic frame reconstructed on-land and offshore (Fig. 13a). Additionally, involvement in folding of young (~200–400 ka) fan deposits along the southern border of Pollino (Figs. 8b and 11), and of the Middle and possibly the Upper Pleistocene seismostratigraphic sequence at its offshore extension (Fig. 13c) makes a strong argument for folding of marine terraces at the intervening coastal strip. The remarkable consistency in trend location and orientation between emerged and submerged areas (Fig. 13a) suggests that the last fold generation mapped in the bedrock was active through the Quaternary and caused deformation of marine terraces and currently persisting fluvial anomalies.

Although analysis of coastal terraces do not precisely constrains the orientation of fold axes, correlation with the younger folds mapped in bedrock on-land (Figs. 8 and 9), and imaged in offshore seismic profiles, together with the elongation of prominent fluvial anomalies (Fig. 6), suggests that the folds affecting the coastal terraces are almost orthogonal to the coastline in the north (Fig. 13 a). In the south, they probably keep slightly oblique to the coastline. At the northeast border of the Sila range, a marked SL index anomaly (Fig. 6), which spatially coincides with a main undulation in marine terrace profiles (Figs. 4 and 5), is in agreement with a similar index and residual topography anomaly reported by Molin et al. (2004). The topography anomaly (OD ridge in Molin et al., 2004) is centered above a structural culmination where meta-sedimentary rocks are exposed in tectonic window beneath Calabrid crystalline rocks (Fig. 13a). Although Molin et al. (2004) suggested footwall uplift along unspecified normal faults as the driving mechanism for deformation we speculate that shortening and transpression along the Corigliano–

Table 3

Parameters of focal solutions for crustal earthquakes in northeastern Calabria

No.	Lon	Lat	Depth (km)	Mw	Date (yyymmdd)	kinematics	Reference ^a
1	16.86	39.9	2.5	3.5	920530	Normal	FA00
2	17.01	39.58	8.6	3.8	930810	Normal	FA00
3	16.86	39.58	7.6	3.2	950815	Thrust	FA00
4	16.71	39.56	10.2	3.4	951202	Normal	FA00
5	16.71	39.35	17.0	4.7 ^b	020417	Strike-slip	RCMT
6	16.98	39.26	12	3.9	070326	Strike-slip	RCMT
7	16.7333	39.4837	18.4	3.5	050423	Normal	Mu07
8	16.7138	39.4872	26.6	4.0	050423	Strike-slip	Mu07
9	17.0798	39.2371	14	3.6	051203	Thrust	Mu07
10	16.4864	39.492	7.9	3.3	051211	Thrust	Mu07
11	17.2223	39.1928	12.3	3.4	060117	Strike-slip	Mu07
12	17.1153	39.5967	12	4.7 ^c	060417	Strike-slip ^d	Mu07
13	16.6338	39.7345	6.8	3.8	060622	Thrust ^d	Mu07
14	16.7991	39.6625	24.6	3.8	070525	Strike-slip	Mu07

^a FA00 = Frepoli and Amato, 2000; RCMT = Mednet Regional Centroid Moment Tensor, INGV; Mu07 = Mucciarelli, 2007.

^b Mb from Mednet RCMT catalogue.

^c MI from Mednet RCMT catalogue.

^d Focal solution and depth from Mednet quick RCMT determination.

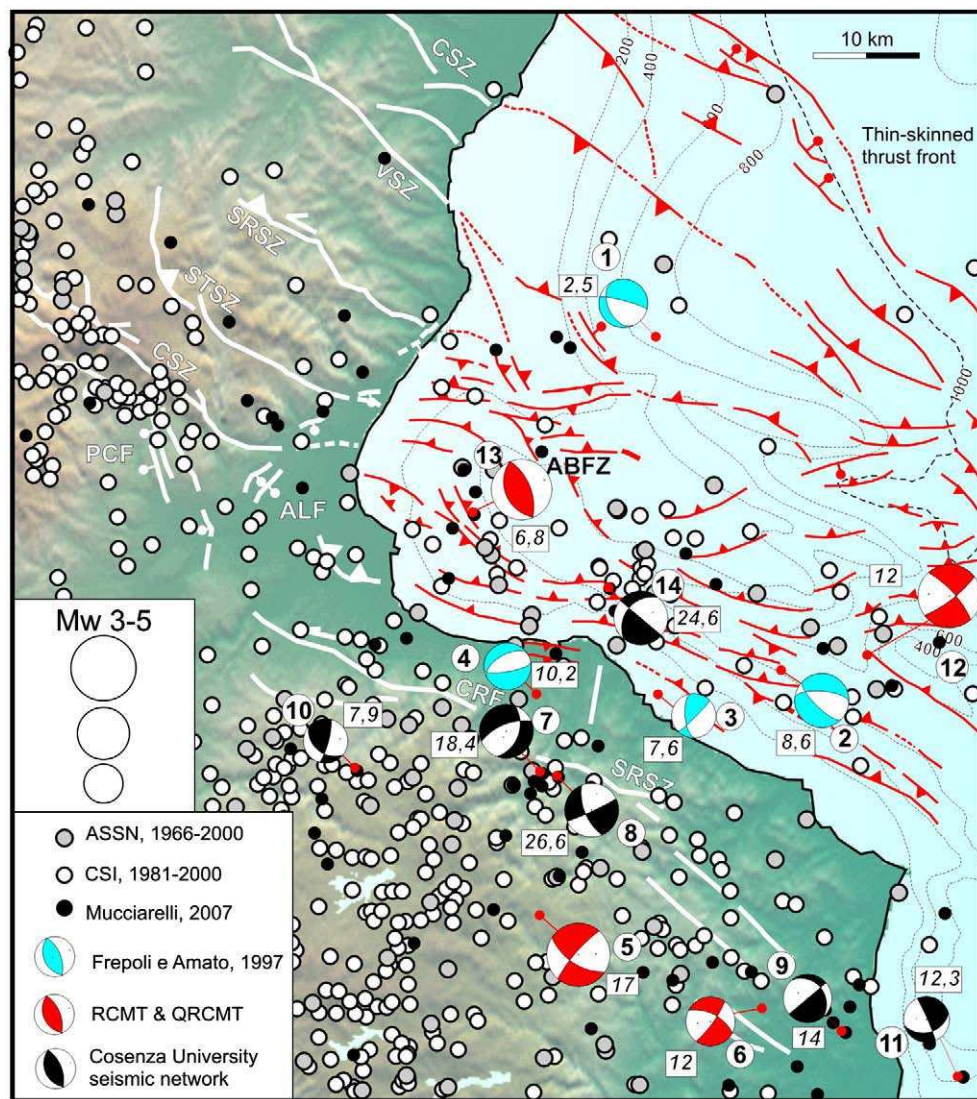


Fig. 14. Seismotectonic setting of northeastern Calabria. White dots are epicenters of 1981–2002 instrumental seismicity from the Istituto Nazionale di Geofisica e Vulcanologia (INGV) database (<http://www.ingv.it/CSI/>); grey dots are epicenters of 1966–2003 instrumental seismicity ($M > 2$) from the Advanced Seismic Station Network (ASSN) database (<http://earthquake.usgs.gov/research/monitoring/anss/>). Focal mechanisms of moderate ($2.3 < M < 4.1$) crustal earthquakes from Frepoli and Amato (2000) (medium grey), Mednet RCMT e QRCMT [1997–2006] (<http://mednet.ingv.it/events/QRCMT/Welcome.html>) catalogue (heavy grey) and this work using data provided by I. Guerra (black). Boxed numbers are depths of focal solutions in km. Circled numbers relate events to parameters listed in Table 3. Faults labeled as in Fig. 3.

Rossano fault was focused at this location, exposing structurally subjacent rocks and still controlling active fold growth.

4.2. Regional tectonic context of the recent folds

The ~E- to ~SE-trending recent folds revealed by integrated analysis of bedrock structures, coastal terraces and fluvial anomalies are consistent with the structural frame of the region reconstructed from surface and subsurface data. Specifically, the origin of these structures appears related to deep-seated imbrication in the Apulian foreland platform underlying the thin-skinned thrust belt.

The structural highs and lows responsible for the morphological anomalies can be traced at depth within the Apulian bedrock (see also Monaco et al., 1998; Catalano et al., 2004). North of Pollino, subsurface thrusts within the Apulian platform based on oil exploration data (Fig. 3) are aligned with the geomorphic anomalies mapped in the study area. East of the Valsinni ridge, these thrusts bound submerged anticlines behind the leading edge of the thin-skinned belt (Fig. 13a). Seismic

profiles document dramatic structural relief of the Apulian platform rocks and their Neogene cover beneath the Amendolara ridge (Fig. 13a), whose southern front accommodates seismologically active transpression (Fig. 14).

Growth of the Apulian structures in the frontal part of the Southern Apennines as constrained by the age of exposed or drilled synorogenic sequences (Patacca and Scandone, 2001) is broadly coeval with onset of marine terraces displacement. Commencement of Valsinni ridge uplift in response to deep imbrication of Apulian platform rocks is bracketed between late Early to earliest Middle Pleistocene (Hippolyte et al., 1994; Patacca and Scandone, 2001). To the west, Middle Pleistocene continental deposits in the Sant'Arcangelo basin are folded around ESE-WNW axes (Fig. 13a; Casciello et al., 2000). A marked sedimentary response to active growth of the Pollino range is recorded by the northward progradation of Middle to Upper Pleistocene fan and alluvial depositional systems on the southern border of the basin (Giannandrea and Loiacono, 2003). This pattern is coeval to, and mirrors the southward growth of, the southern side of the range (Fig. 8b) and of its offshore extension (Fig. 13c).

In summary, growth of the Pollino–Valsinni–Amendolara ridges was largely controlled by deep-seated transpression in the Apulian platform buried beneath the thin-skinned belt. Post-Early Pleistocene shortening was coeval to rapid surface uplift, and is recorded by tilting and folding of deposits and terraces and by a range of geomorphic anomalies. Whereas on the northern side of the Pollino–Valsinni ridges displacement appears directed toward the northeast, structural asymmetry on the southern border of Pollino and Amendolara ridge and at the northern Sila coastline indicates southwest-directed tectonic transport during Quaternary.

4.3. Significance of extensional slip on the Avena–Lauropoli fault

Although observations of the Avena–Lauropoli fault were sparsely made by previous workers (Lanzafame and Tortorici, 1981; Ambrosetti et al., 1987; Hippolyte et al., 1992; Cucci and Cinti, 1998; Bentivenga et al., 2004b), few details were available to date on the fault geometry and kinematics, and its existence was questioned by Cucci (2004). In agreement with Lanzafame and Tortorici (1981) and Hippolyte et al. (1992), our detailed mapping documents a main extensional slip, but also indicates that the fault is not through-going. This observation is consistent with the argument that, within a regional transpressional displacement field, slip on the Avena–Lauropoli fault is unlikely to reflect deep crustal stretching as observed elsewhere in the Apennines. The NW–SE extension resolved on this fault (Fig. 10) is kinematically incompatible with the regional NE–SW crustal extension found to the west in the Apennines chain, but would be compatible with the extension direction recorded in the Calabrian arc (Fig. 2). However, clear seismological and geological evidence of extension is found on the western side of Calabria, but lacks further east. Besides, normal faulting is segregated on the eastern, low-lying flank of Pollino and in its offshore, and does not penetrate in the interior of the mountain range (Fig. 10).

Field observations document locally dramatic bedding tilts on moderately-dipping fault surfaces of the Avena–Lauropoli array (Fig. 12a and c), which are consistent with a relatively shallow depth-to-detachment. Differential uplift across the coastline, which peaks in the interior of the mountain belt, is inquired as triggering dip-slip on the Avena–Lauropoli fault. When individual strands of the fault are seen in the context of distributed transpressional deformation in the Pollino range, their segmented pattern may indicate the lateral extent of differential uplift compartments controlled by individually growing folds and thrusts (Fig. 13a). It is unknown whether the ~50 m cumulative vertical slip retrieved on the fault during the last ~200 ka was linearly accrued or rather occurred during few catastrophic events. Consistency of displacement budget along the fault trace (Fig. 5), however, suggests that creeping was likely.

This situation is not unique to the Pollino range. As a matter of fact, shallow-rooted listric normal faults are mapped offshore along the flanks of the Amendolara and of the frontal ridge (Fig. 13b), suggesting gravitational collapse toward the Sinni and Bradano basins. A cohort of more localized gravitational phenomena possibly related to slip on these and other normal faults were imaged in previous marine geophysical surveys (Rossi and Gabbianelli, 1978; Rossi et al., 1983). It appears that the listric faults imaged offshore detach above the Lower Pleistocene reflector (Fig. 13b). This horizon is exposed on-land as a continuous clay package, and thus rooting of the collapsed panels at this level is no surprise and supports a creeping mechanism.

On a similar fashion, Bentivenga et al. (2004a,b) argued that gravitational collapse of a single regional terrace in the Bradano basin has recently occurred toward the Taranto Gulf on several sets of NE–SW striking faults. Unlike Bentivenga et al. (2004a,b), however, we contend that the conditions for gravitational collapse in our study area were set by transpressional uplift concentrated in the interior of the mountain belt, and unevenly affected portions of a well-developed terrace flight.

4.4. Seismotectonic frame

Involvement in folding of young marine terraces and recent sediments points to current shortening accommodated in this region. The moderate seismicity is consistent with thrusting and strike-slip motion partitioned within sub-parallel, NW–SE trending transpressional belts south of the Amendolara ridge and on the northern side of Sila (Fig. 13a). Although a mixture of focal solutions is recorded in the area, the *P*-axes of earthquakes trend systematically from ~ESE to ~ENE (Fig. 14). The *T*-axes trends from NW–SE to ~N–S. It appears that a permutation between the minimum and intermediate principal incremental strain axes occurs, so that transpression is partitioned between thrust and strike-slip motions. Locally, the maximum and intermediate incremental strain axes also exchange, and extensional slip is recorded. In light of the regional shortening, the extensional focal solutions observed around Capo Trionto (Fig. 14) might reflect collapse and lateral stretching of deep growing anticlines, or negative flower structures at releasing bends. The seismological normal faulting also agrees with the pattern of slumping and creeping of near-surface sediments evidenced on-land (Fig. 12) and offshore (Fig. 13b).

The trend of seismic axes is to a large degree consistent with the orientation of the finite displacement field as determined by structural and fault-slip analysis in recent deposits. A Middle Pleistocene ~ENE trending shortening axis for transpressional faults is retrieved at the eastern flank of Pollino (Fig. 10), and is sub-parallel to the *P*-axes of thrust and strike-slip earthquakes just to the southeast in the Amendolara and northern Sila seismic belts. On the other hand, Middle Pleistocene N–S to NW–SE trending shortening is found on the southern border of the range (Fig. 10), but comparison with the incremental strain field is hindered there by the lack of seismic events.

The seemingly odd divergence in the finite and incremental strain axes orientation moving from Pollino to Sila is, however, in agreement with geodetic velocity residuals. When viewed in a MATE reference frame, GPS velocities of sites in southern Pollino converge toward MATE indicating ~N–S shortening in the intervening region (Fig. 3), a pattern consistent with that documented in Middle Pleistocene rocks (Fig. 10). On the other hand, a site on the Sila massif converge obliquely toward MATE and its velocity is sub-parallel to the *P*-axes of earthquakes in the southern Taranto Gulf (Figs. 3 and 14). Thus, conditions of non-plane strain are achieved in the region, consistent with active transpression.

Integration of surface velocity and fault studies, seismicity and seismic profiles indicates that active shallow-crustal folding reflects deeper shortening. Thrust and transpressional earthquakes occur both in the deep Apulian sedimentary and crystalline crust beneath ~10–15 km depth, and in the overlying accretionary wedge. The spatial distribution of epicenters of crustal earthquakes and the incremental strain axes provided by focal mechanisms in the study area, together with GPS velocities, are consistent with the location and trace of the major morphotectonic and bedrock transpressional faults (Fig. 14).

Uncertainty, however, surrounds the existence of active motion on the transpressional shear zones mapped on-land and having a main Early Pleistocene activity (Catalano et al., 1993; Monaco et al., 1998). Given the lack of co-seismic and paleoseismological evidence of transpressional faulting in the Pollino range, the folding mechanism is not yet established. Although the folds mapped in coastal terraces might reflect transpressional slip on the mapped ~NW–SE striking faults, evidence of brittle deformation within the marine deposits is weak. Thus, it is still unresolved whether the folded terraces reflect parasitic trains related to a regional buckling or fault-related folds, or both. The offshore extension of the Satanasso shear zone coincides with a major fault-related fold in Middle–Upper Quaternary sediments (Larissa High, Fig. 13c), and thus the Satanasso fault may be currently slipping at depth.

Within the Sibari basin, a thrust earthquake activated the offshore extension of the Civita shear zone (Fig. 14). Thus, some cases may exist for local transpressional fault-related folding in a belt which stretches ~80–100 km from southern Pollino in the west to the eastern termination of the Amendolara ridge in the east. The belt appears composed of individual strands of maximum length <15 km, placing limits on the maximum expected earthquake size.

4.5. Regional tectonic implications

The discovery of an active back-directed transpressional belt on the Ionian Sea side of northern Calabria has profound implications for models of active orogenic deformation in southern Italy. Because of the lack of significant-sized seismicity, this region is commonly considered a stable block captured between the active extensional belt of the Apennines and the Hellenic–Dinaric thrust front in the eastern Adriatic Sea (Fig. 2; Montone et al., 2004). This interpretation relies on the notion provided by regional stratigraphic and tectonic analysis that motion of the thin-skinned thrust front ceased by the onset of Middle Pleistocene (Patacca et al., 1990; Hippolyte et al., 1994; Patacca and Scandone, 2001). On the other hand, GPS velocities and, locally, moderate-sized seismicity are consistent with active transpression in the east adjacent to the active extensional belt of the western Apennines (Ferranti et al., 2008). In light of regional GPS velocity patterns, fault slip studies in recent rocks, geomorphic analysis and seismic reflection profiles, it can be argued that the transpressional belt likely involves the whole eastern part of Lucania–Calabria Apennines and of the Bradano basin.

We speculate that the folds mapped in coastal terraces together with fluvial geomorphic anomalies are upper crustal effects of shear zones splaying from the basal detachment of the transpressional belt. Published subsurface data in the region do not allow to infer the depth of the detachment, which must be deeper than the frontal thrust of the Miocene–Pliocene thin-skinned belt (Fig. 13b; see also Van Dijk et al., 2000). The seismic profile across the Amendolara ridge (Fig. 13b) shows the transpressional faults rooting at depths larger than 5 sec TWT, which, assuming reasonable rock velocities, corresponds to ~10 km depth. Similarly, a regional seismic section located ~100 km southeast of, and on the sea-ward projection of the Amendolara ridge shows the thin-skinned belt cut by back-thrusts emanating from a ≥ 7 km depth (Doglioni et al., 1999). A crustal section across northern Calabria and the southern Taranto Gulf reconstructed from field and subsurface data analysis shows transpressional shear zones emanating from a depth of nearly 20 km through the Apennines accretionary prism and underlying Apulian plate (Van Dijk et al., 2000).

Moderate thrust and strike-slip earthquakes are found at depths of up to ~25 km (Fig. 14), which is near the base of the crust (Cassinis et al., 2003). Processes occurring at deep-crustal or sub-crustal depth sustain the regional uplift of the Calabrian arc (Westaway, 1993; Wortel and Spakman, 2000; Gvirtzman and Nur, 2001), but shallow (local) and deep (regional) effects are probably coupled (e. g. Bertotti et al., 2001; Ferranti and Oldow, 2005). Whereas in the western side of the Calabrian arc local sources to total uplift are represented by extensional faults, and both regional and local sources are demonstrably coupled (Westaway, 1993; Ferranti et al., 2007), the situation in eastern southern Italy is different. Here, as this study shows, local sources are represented by folds and transpressional faults, which may account for at least one third to one fourth of the total uplift. Although the origin of regional uplift is debated (Wortel and Spakman, 2000; Gvirtzman and Nur, 2001; Westaway and Bridgland, 2007), the coupling between shallow and deep sources points to wholesale crustal and lithospheric folding (Bertotti et al., 2001; Ferranti and Oldow, 2005) as a viable contributor to the large-scale uplift of the eastern side of southern Italy.

Localization of the transpressional belt in northeastern Calabria may be related to the existence of long-lived crustal or lithospheric boundaries. Based on seismicity and modelling of regional profiles, it appears that the transpressional belt is rooted at lower crustal depths, where the transition between the Adriatic continental crust and the Ionian thinned continental or oceanic crust occurs (Fig. 1b). This deep boundary crosses peninsular Italy right beneath northeastern Calabria, and development of the back-directed transpressional belt therein is not fortuitous. Likely, the extreme mechanical interface between different crusts has focused the growth of the back-thrust transpressional belt when Adria–Europe relative motion prevailed over the thin-skinned thrust belt propagation during slow-down of the Adriatic–Ionian slab retreat.

5. Conclusions

Although motion of the thrust front in the Southern Apennines orogen waned by the Middle Pleistocene, contraction is still ongoing and is distributed behind the front of the thin-skinned thrust belt. Shortening is manifested by small wavelength and small amplitude undulations which are pervasively summed to the regional uplift profile of Middle–Late Pleistocene marine terraces on the Ionian Sea coast of northern Calabria, stretching from northern Sila to Pollino ranges. When evaluated in light of the seismotectonic frame of the region reconstructed through tectonic and seismicity analysis, the origin of these local anomalies in the deformation profile is reconciled with shallow-crustal anticline and syncline trains related to a recent and still active transpressional field.

Quantitative analysis of streams flowing toward this coastline reveals the existence of ~E–W to NW–SE striking anomaly axes, which spatially coincides with the last generation of folds mapped in the bedrock. On both the northern and the southern flank of the Pollino range, folds with similar trend involve late Middle Pleistocene sediments, and their trace intersects the marine terraces undulations at the coast. On the offshore extension of these structures, the late Middle Pleistocene sedimentary sequence is tilted and folded and the sea-bottom topography is controlled by SW-directed high-angle oblique thrust faults which cut across the early low-angle, NE-directed thrust imbricates.

The young transpressional structures are related to deep-seated shear zones that involve the Apulian foreland plate underlying the thin-skinned accretionary wedge. Arrays of NW–SE striking faults which were previously mapped in northern Calabria, may be traced in the offshore through seismic reflection profiles analysis, forming an at least 100 km long belt of back-directed transpression rooted at depths larger than 10–15 km and involving limited-length segments. Folding of terraces and fluvial anomalies may be related to deep shear along these faults, although a contribution from larger-scale crustal buckling may not be discarded. Local, fault-related sources are strongly coupled to the deep sources, pointing to whole crustal shortening as a possible contributor to regional uplift in this sector of the Calabrian arc.

Although this region was regarded as a stable and almost aseismic block, the deep-seated shear zones do have a seismologic expression. Two NW–SE trending seismic belts are illuminated by epicenters of instrumental earthquakes. Moderate magnitude thrust and strike-slip earthquakes are distributed along the southern escarpment of the Amendolara ridge, which forms the offshore extension of the Pollino range. A parallel transpressional seismic belt is found to the south in the northern Sila massif and spatially coincides with mapped left-transpressional faults. Focal solutions indicate that partitioning between thrust and left-strike-slip motion occurs along the deep-seated shear zones in response to ~E to NE directed shortening. Minor extensional events are related to near-surface slumping and/or releasing bends of the master faults. Microtectonic analysis in recent

sediments along the southern border of Pollino indicates ~N–S shortening. Both the ENE–WSW and the N–S shortening recorded in the eastern and western part of the study area, respectively, are sub-parallel to GPS velocity residuals, and are consistent with active transpression.

On the coastal fringe of Pollino, the Avena–Laupoli normal fault is not through-going and slip is accompanied by locally dramatic stratal tilting, indicative of rooting at shallow depths. We argue that slip locally occurs in response to differential uplift in the interior of the mountain range. Similar situations are evident in seismic profiles, with near-surficial slumping associated to actively growing transpressional ridges underneath.

The novel seismotectonic frame reconstructed for this region carries the implication that a substantial fraction of the geodetic shortening detected between the Pollino and Sila mountain ranges and the Apulian block might be accommodated here. Although this part of the central Mediterranean region is at present one of relatively low-rate displacement, our study allows to reconcile contemporary deformation to the long-term tectonic architecture, pointing to the capability of capturing orogenic deformation by integration of

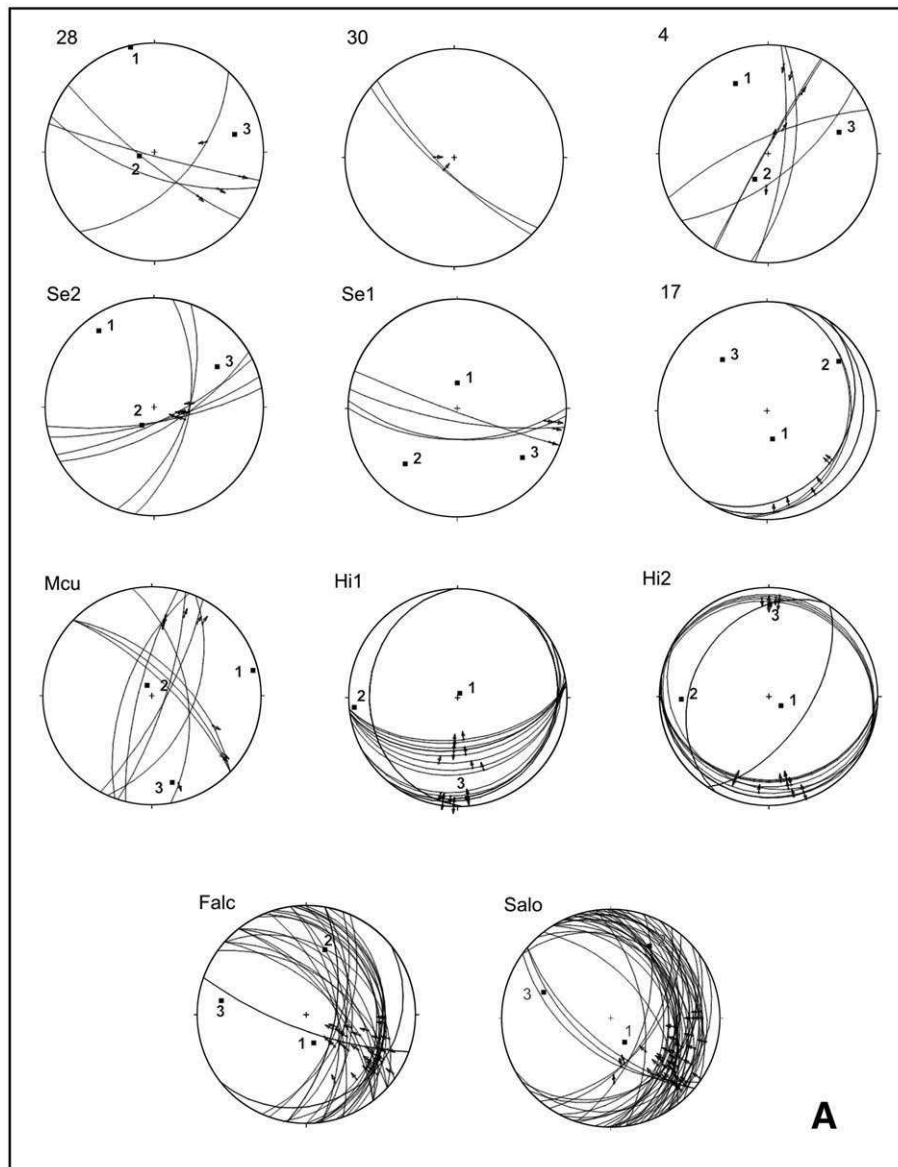
morphotectonic markers, structural and seismicity analysis, and geodetic velocities.

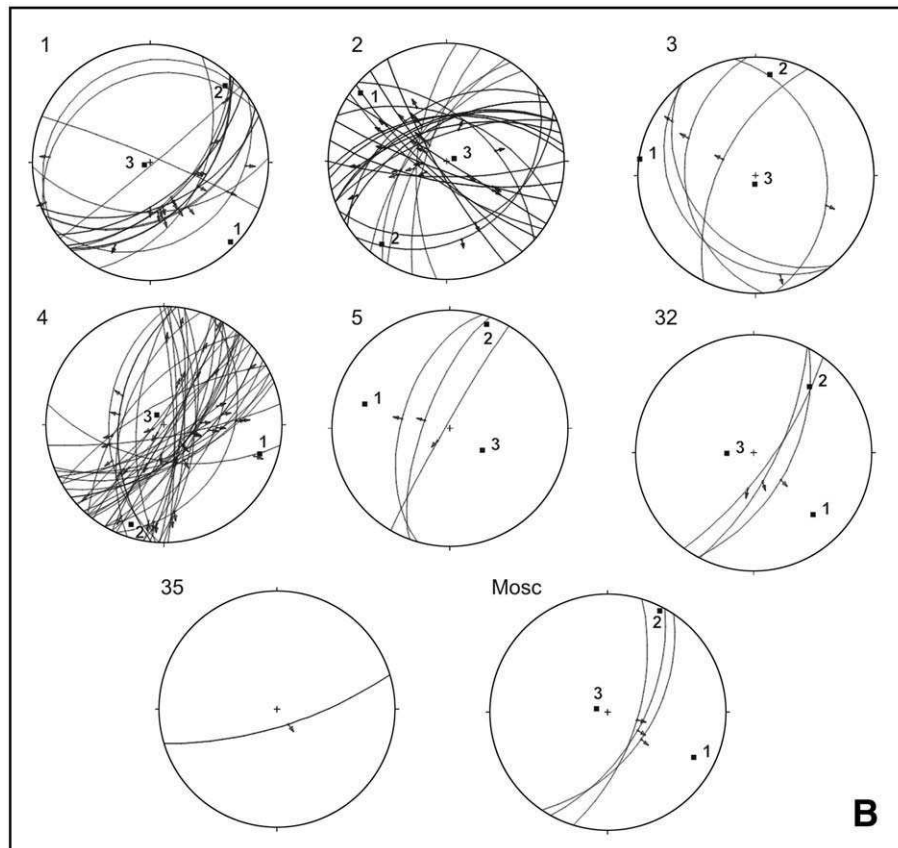
Acknowledgements

U. Radtke and S. Rittner are acknowledged for providing preliminary results of ESR dating of shells. The focal mechanisms of Mucciarelli (2007) were made available by the local network of Cosenza University (courtesy of I. Guerra). This work was funded by PRIN 2005 and DPC-INGV 2007–2009 grants to L. F.

Appendixes A and B

Lower-hemisphere, Wulff projections of fault kinematic data measured at each site located in Fig. 10. Arrows on fault planes indicate motion of the hanging-wall block. Squares labeled 1, 2 and 3 are kinematic axes calculated at each site using software Faultkin 1.2 (Marrett and Allmendinger, 1990): 1, maximum tension; 2, intermediate tension; 3, minimum tension (compression). A) Transpressional fabrics; B) Extensional fabrics





References

- Amato, A., Montone, P., 1997. Present-day stress field and active tectonics in southern peninsular Italy. *Geophys. J. Int.* 130, 519–534.
- Ambrosetti, P., Bartolini, C., Bosi, C., Carraro, F., Ciaranfi, F.N., Panizza, M., Papani, G., Vezzani, L., Zangheri, A., 1987. Neotectonic Map of Italy (Scale 1:500,000). Consiglio Nazionale delle Ricerche, Progetto Finalizzato Geodinamica, Rome, Italy.
- Anderson, H., Jackson, J., 1987. Active tectonics of the Adriatic region. *Geophys. J. R. Astron. Soc.* 91, 937–983.
- Bassinot, F.C., Labeyrie, L.D., Vincent, E., Quidelleur, X., Shackleton, N.J., Lancelot, Y., 1994. The astronomical theory of climate and the age of the Brunhes–Matuyama magnetic reversal. *Earth Planet. Sci. Lett.* 126, 91–108.
- Bentivenga, M., Coltorti, M., Prosser, G., Tavarnelli, E., 2004a. A new interpretation of terraces in the Taranto Gulf: the role of extensional faulting. *Geomorphology* 60, 383–402.
- Bentivenga, M., Coltorti, M., Prosser, G., Tavarnelli, E., 2004b. Deformazioni distensive recenti nell'entroterra del golfo di Taranto: implicazioni per la realizzazione di un deposito geologico per scorie nucleari nei pressi di Scanzano Ionico (Basilicata). *Boll. Soc. Geol. Ital.* 123, 391–404.
- Bertotti, G., Picotti, V., Chilovi, C., Fantoni, R., Merlini, S., Mosconi, A., 2001. Neogene to Quaternary sedimentary basins in the south Adriatic (Central Mediterranean): foredeeps and lithospheric buckling. *Tectonics* 20, 771–787.
- Bianca, M., Caputo, R., 2003. Analisi morfotettonica ed evoluzione quaternaria della Val d'Agri, Appennino meridionale. *Il Quaternario* 16, 158–170.
- Bigi, G., Bonardini, G., Catalano, R., Cosentino, D., Lentini, F., Parlotto, M., Sartori, R., Scandone, P., Turco, E., 1992. Structural Model of Italy, 1:500,000. Consiglio Nazionale delle Ricerche, Rome.
- Bonardi, G., Cavazza, W., Perrone, V., Rossi, S., 2001. Calabria–Peloritani Terrane and Northern Ionian Sea. In: Vai, G.B., Martini, I.P. (Eds.), *Anatomy of an Orogen: The Apennines and Adjacent Mediterranean Basins*. Kluwer Academic Publishers, Dordrecht, pp. 287–306.
- Bordoni, P., Valensise, G., 1998. Deformation of the 125 ka marine terrace in Italy: tectonic implications. In: Stewart, I.S., Vita-Finzi, C. (Eds.), *Coastal Tectonics*. Geological Society Special Publication, vol. 146, pp. 71–110.
- Casciello, E., Cesarano, M., Ferranti, L., Oldow, J.S., Pappone, G., 2000. Pleistocene non-coaxial fold development in the northern portion of the S. Arcangelo Basin (Southern Apennines). *Mem. Soc. Geol. Ital.* 55, 133–140.
- Casero, P., Roure, R., Endignoux, L., Moretti, I., Muller, C., Sage, L., Vially, R., 1992. Neogene geodynamic evolution of Southern Apennines. *Mem. Soc. Geol. Ital.* 41, 109–120.
- Cassinis, R., Scarascia, S., Lozej, A., 2003. The deep crustal structure of Italy and surrounding areas from seismic refraction data. A new synthesis. *Boll. Soc. Geol. Ital.* 122, 365–376.
- Catalano, S., Monaco, C., Tortorici, L., Tansi, C., 1993. Pleistocene strike-slip tectonics in the Lucanian Apennine (Southern Italy). *Tectonics* 12, 656–665.
- Catalano, R., Doglioni, C., Merlini, S., 2001. On the Mesozoic Ionian Basin – *Geophys. J. Int.* 144, 49–64.
- Catalano, S., Monaco, C., Tortorici, L., Paltrinieri, W., Steel, N., 2004. Neogene–Quaternary tectonic evolution of the Southern Apennines. *Tectonics* 23. doi:10.1029/2003TC001512TC2003.
- Cello, G., Mazzoli, S., 1999. Apennine tectonics in southern Italy: a review. *J. Geodyn.* 27, 191–211.
- Cello, G., Guerra, I., Tortorici, L., Turco, E., 1982. Geometry of the neotectonic stress field in southern Italy: geological and seismological evidence. *J. Struct. Geol.* 4, 385–393.
- Cesarano, M., Pierantoni, P.P., Turco, E., 2002. Structural analysis of the Albidona Formation in the Alessandria del Carretto–Plataciara area (Calabro–Lucanian Apennines, Southern Italy). *Boll. Soc. Geol. Ital.* 11, 669–676.
- Cinti, F.R., Cucci, L., Pantosti, D., D'Addezio, G., Meghraoui, M., 1997. A major seismogenic fault in a “silent area”: the Castrovillari Fault (southern Apennines, Italy). *Geophys. J. Int.* 130, 595–605.
- Colella, A., Cappadona, P., 1988. Evidenze stratigrafiche del carattere trascorrente sinistro della zona di faglie del Pollino. Valutazione della velocità di trascorrenza. *Atti 74 Congresso Soc. Geol. It.*, 147–150.
- Cucci, L., 2004. Raised marine terraces in the Northern Calabrian Arc (Southern Italy): a ~600 Kyr-long geological record of regional uplift. *Ann. Geophys.* 47, 1391–1406 August 2004.
- Cucci, L., Cinti, F.R., 1998. Regional uplift and local tectonic deformation recorded by the Quaternary marine terraces on the Ionian coast of northern Calabria (southern Italy). *Tectonophysics* 292, 67–83.
- D'Agostino, N., Selvaggi, G., 2004. Crustal motion along the Eurasia–Nubia plate boundary in the Calabrian Arc and Sicily and active extension in the Messina Straits from GPS measurements. *J. Geophys. Res.* 109, B11402. doi:10.1029/2004JB002998.
- Dai Pra, G., Hearty, P.J., 1988. I livelli marini pleistocenici del Golfo di Taranto. Sintesi geocronostratigrafica e tettonica. *Mem. Soc. Geol. Ital.* 41, 637–644.
- Del Ben, A., Barnaba, C., Toboga, A., 2007. Strike-slip systems as the main tectonic features in the Plio–Quaternary kinematics of the Calabrian Arc. *Mar. Geophys. Res.* doi:10.1007/s11001-007-9041-6.
- Doglioni, C., Merlini, S., Cantarella, G., 1999. Foredeep geometries at the front of the Apennines in the Ionian Sea (central Mediterranean). *Earth Planet. Sci. Lett.* 168, 243–254.
- Faccenna, C., Becker, T.W., Lucente, F.P., Jolivet, L., Rossetti, F., 2001. History of subduction and back-arc extension in the Central Mediterranean. *Geophys. J. Int.* 145, 809–820.

- Fairbanks, R.G., Mortlock, R.A., Chiu, T.C., Cao, L., Kaplan, A., Guilderson, T.P., Fairbanks, T.W., Bloom, A.L., 2005. Marine Radiocarbon Calibration Curve Spanning 0 to 50,000 Years B.P. Based on Paired $^{230}\text{Th}/^{234}\text{U}/^{238}\text{U}$ and ^{14}C Dates on Pristine Corals. *Quat. Sci. Rev.* 24, 1781–1796.
- Ferranti, L., Oldow, J.S., 2005. Latest Miocene to Quaternary horizontal and vertical displacement rates during simultaneous contraction and extension in the Southern Apennines orogen, Italy. *Terra Nova* 17, 209–214.
- Ferranti, L., Antonioli, F., Mauz, B., Amorosi, A., Dai Prà, G., Mastronuzzi, G., Monaco, C., Orrù, P., Pappalardo, M., Radtke, U., Renda, P., Romano, P., Sansò, P., Verrubbi, V., 2006. Markers of the last interglacial sea-level high stand along the coast of Italy: tectonic implications. *Quat. Int.* 145–146, 30–54.
- Ferranti, L., Monaco, C., Antonioli, F., Maschio, L., Kershaw, S., Verrubbi, V., 2007. The Contribution of Regional Uplift and Coseismic Slip to the Vertical Crustal Motion in the Messina Straits, Southern Italy: Evidence from Raised Late Holocene Shorelines. *Journal of Geophysical Research*, vol. 112, p. B06401. doi:10.1029/2006JB004473.
- Ferranti, L., Oldow, J.S., D'Argenio, B., Catalano, R., Lewis, D., Marsella, E., Avellone, G., Maschio, L., Pappone, G., Pepe, F., Sulli, A., 2008. Active deformation in Southern Italy, Sicily and southern Sardinia from GPS velocities of the Peri-Tyrrhenian Geodetic Array (PTGA). *Boll. Soc. Geol. It.* (Ital. J. Geosci.), 127/2, 299–316.
- Frepoli, A., Amato, A., 2000. Fault plane solutions of crustal earthquakes in Southern Italy (1988–1995): seismotectonic implications. *Ann. Geophys.* 43 (3), 437–468.
- Friedrich, A.M., Wernicke, B.P., Niemi, N.A., Bennett, R.A., Davis, J.L., 2003. Comparison of geodetic and geologic data from the Wasatch region, Utah, and implications for the spectral character of Earth deformation at periods of ten to ten million years. *J. Geophys. Res.* 108, 2199. doi:10.1029/2001JB000682.
- Galadini, F., Meletti, C., Rebez, A., 2000. (A cura di), Le ricerche del GNDT nel campo della pericolosità sismica (1996–1999), CNR-Gruppo Nazionale per la Difesa dai Terremoti – Roma, 2000, 397 pp.
- Galli, P., Bosi, V., 2003. Catastrophic 1638 earthquakes in Calabria (southern Italy). New insight from paleoseismological investigation. *J. Geophys. Res.* 108B1. doi:10.1029/2002JB01713.
- Gasparini, C., Iannaccone, G., Scarpa, R., 1985. Fault-plane solutions and seismicity of the Italian Peninsula. *Tectonophysics* 117, 59–78.
- Giannandrea, P., Loiacono, F., 2003. Le successioni alluvionali e lacustri Quaternarie affioranti nella media valle del Fiume Sinni (Appennino meridionale, Basilicata). *Il Quaternario* 16, 257–267.
- Goes, S., Giardini, D., Jenny, S., Hollenstein, C., Kahle, H.G., Geiger, A., 2004. A recent tectonic reorganization in the south-central Mediterranean. *Earth Planet. Sci. Lett.* 226, 335–345.
- Gueguen, E., Doglioni, C., Fernandez, M., 1998. On the post-25 Ma geodynamic evolution of the western Mediterranean. *Tectonophysics* 298, 259–269.
- Gvirtzman, Z., Nur, A., 2001. Residual topography, lithospheric structure and sunken slabs in the central Mediterranean. *Earth Planet. Sci. Lett.* 187, 117–130.
- Hollenstein, C., Kahle, H.G., Geiger, A., Jenny, S., Goes, S., Giardini, D., 2003. New GPS constraints on the Africa–Eurasia plate boundary in southern Italy. *Geophys. Res. Lett.* 30, 1935. doi:10.1029/2003GL017554.
- Hunstad, I., Selvaggi, G., D'Agostino, N., England Clarke, P., Pierozzi, M., 2003. Geodetic strains in peninsular Italy between 1875 and 2001. *Geophys. Res. Lett.* 30, 1828. doi:10.1029/2002GL016447.
- Hippolyte, J.C., Angelier, J., Roure, F., 1992. Les permutations d'axes de contraintes dans des terrains quaternaires du sud de l'Apennin (Italie). *C. R. Acad. Sci., Paris* 315, 89–95.
- Hippolyte, J.C., Angelier, J., Roure, F., 1994. A major geodynamic change revealed by Quaternary stress patterns in the Southern Apennines (Italy). *Tectonophysics* 230, 199–210.
- King, G.C.P., Stein, R.S., Rundle, J.B., 1988. The growth of geological structures by repeated earthquakes 1. Conceptual framework. *J. Geophys. Res.* 93, 13307–13318.
- Knott, S.D., Turco, E., 1991. Late Cenozoic kinematics of the Calabrian Arc, southern Italy. *Tectonics* 10, 1164–1172.
- Lanzafame, G., Tortorici, L., 1981. La tettonica recente della Valle del fiume Crati (Calabria). *Geogr. Fis. Din. Quat.* 4, 11–21.
- Malinverno, A., Ryan, W.B.F., 1986. Extension in the Tyrrhenian Sea and shortening in the Apennines as a result of arc migration driven by sinking of the lithosphere. *Tectonics* 5, 227–245.
- Marrett, R., Allmendinger, R.W., 1990. Kinematic analysis of fault-slip data. *J. Struct. Geol.* 12, 973–986.
- Maschio, L., Ferranti, L., Burrato, P., 2005. Active extension in Val d'Agri area, Southern Apennines, Italy: implications for the geometry of the seismogenic belt. *Geophys. J. Int.* 162, 591–609. doi:10.1111/j.1365-246X.2005.02597.x.
- Menardi-Noguera, A., Rea, G., 2000. Deep structure of the Campanian–Lucanian Arc (Southern Apennine, Italy). *Tectonophysics* 324, 239–265.
- Miyauchi, T., Dai Pra, G., Sylos Labini, S., 1994. Geochronology of Pleistocene marine terraces and regional tectonics in the Tyrrhenian coast of South Calabria, Italy. *Il Quaternario* 7, 117–134.
- Molin, P., Pazzaglia, F.J., Dramis, F., 2004. Geomorphic expression of active tectonics in a rapidly-deforming forearc, Silamassif, Calabria, southern Italy. *Am. J. Sci.* 304, 559–589.
- Monaco, C., 1993. Pleistocene strike-slip tectonics in the Pollino mountain range (Southern Italy). *Ann. Tecton.* 8/2, 100–112.
- Monaco, C., Tortorici, L., 2000. Active faulting in the Calabrian arc and eastern Sicily. *J. Geodyn.* 29, 407–424.
- Monaco, C., Tortorici, L., Paltrinieri, W., 1998. Structural evolution of the Lucanian Apennines, southern Italy. *J. Struct. Geol.* 20, 617–638.
- Montone, P., Mariucci, M.T., Pondrelli, S., Amato, A., 2004. An improved stress map for Italy and surrounding regions (Central Mediterranean). *J. Geophys. Res.* 109, 10410. doi:10.1029/2003JB002703.
- Mucciarelli, M., 2007. Rendicontazione conclusiva, UR 2.12. In: Galadini, F. (Ed.), Definizione spaziale delle principali strutture sismogenetiche della penisola italiana, Progetti sismologici di interesse per il DPC, pp. 225–234.
- Oldow, J.S., Ferranti, L., 2006. Fragmentation of Adria and active decollement tectonics within the southern peri-Tyrrhenian orogen, Italy. In: Pinter, N., Gyula, G., Weber, J., Stein, S., Medak, D. (Eds.), The Adria Microplate: GPS Geodesy, Tectonics, and Hazards. NATO Science Series IV, vol. 61. Springer, pp. 269–286.
- Oldow, J.S., Ferranti, L., Lewis, D., Campbell, L., D'Argenio, B., Catalano, R., Pappone, G., Carmignani, L., Conti, P., Aiken, C., 2002. Active fragmentation of Adria, the north African promontory, central Mediterranean orogen. *Geology* 30, 779–782.
- Patacca, E., Scandone, P., 2001. Late thrust propagation and sedimentary response in the thrust belt-foredeep system of the Southern Apennines (Pliocene–Pleistocene). In: Vai, G.B., Martini, I.P. (Eds.), Anatomy of a Mountain Belt: the Apennines and Adjacent Mediterranean Basins. Kluwer Academic Publishers, pp. 401–440.
- Patacca, E., Sartori, R., Scandone, P., 1990. Tyrrhenian Basin and Apenninic arcs: kinematic relations since late Tortonian times. *Mem. Soc. Geol. Ital.* 45, 425–451.
- Pieri, P., Vitale, G., Benedice, P., Dogliosi, C., Gallicchio, S., Giano, S.I., Loizzo, R., Moretti, M., Prosser, G., Sabato, L., Schiattarella, M., Tramutoli, M., Tropeano, M., 1997. Tettonica quaternaria nell'area Bradanico-Ionica. *Il Quaternario* 10, 535–542.
- Randisi, A., 2007. Evoluzione morfotettonica tardo-quaternaria della Piana di Sibari, Calabria settentrionale. Tesi di dottorato, Scienza e Ingegneria del Mare, Naples, 162 pp.
- Rossi, S., Gabbianelli, G., 1978. Geomorfologia del golfo di Taranto. *Boll. Soc. Geol. Ital.* 97, 423–437.
- Rossi, S., Aurox, C., Mascle, J., 1983. The Gulf of Taranto (Southern Italy): seismic stratigraphy and shallow structure. *Marine Geology* 51, 327–346.
- Roure, F., Casero, P., Vially, R., 1991. Growth process and mélange formations in the Southern Apennines accretionary wedge. *Planet. Sci. Lett.* 102, 395–412.
- Santoro, E., Mazzella, M.E., Ferranti, L., Randisi, A., Napolitano, E., Rittner, S., Radtke, U., 2009. Raised coastal terraces along the Ionian Sea coast of northern Calabria, Italy, suggest space and time variability of tectonic uplift rates. *Quat. Int.*
- Selvaggi, G., Chiarabba, C., 1995. Seismicity and P-wave velocity image of the southern Tyrrhenian subduction zone. *Geophys. J. Int.* 121, 818–826.
- Tansi, C., Muto, F., Critelli, S., Iovine, G., 2007. Neogene–Quaternary strike-slip tectonics in the central Calabrian Arc (southern Italy). *J. Geodyn.* 43, 393–414.
- Van Dijk, J.P., Bello, M., Brancaloni, G.P., Cantarella, G., Costa, V., Frixia, A., Golfetto, F., Merlini, S., Riva, M., Torricelli, S., Toscano, C., Zerilli, A., 2000. A regional structural model for the northern sector of the Calabrian Arc (southern Italy). *Tectonophysics* 324, 267–320.
- Vezzani, L., 1968. I terreni plio-pleistocenici del basso Crati (Cosenza). *Atti Accademia Gioenia Scienze Naturali, Catania*, 6/20, 28–84.
- Waelbroeck, C., Labeyrie, L., Michel, E., Duplessy, J.C., Lambeck, K., McManus, J.F., Balbon, E., Labracherie, M., 2002. Sea level and deep water temperature changes derived from benthic foraminifera isotopic records. *Quat. Sci. Rev.* 21, 295–305.
- Westaway, R., 1993. Quaternary uplift of southern Italy. *J. Geophys. Res.* 87, 21741–21772.
- Westaway, R., Bridgland, D., 2007. Late Cenozoic uplift of southern Italy deduced from fluvial and marine sediments: coupling between surface processes and lower-crustal flow. *Quat. Int.* 175, 86–124.
- Wortel, M.J.R., Spakman, W., 2000. Subduction and slab detachment in the Mediterranean–Carpathian region. *Science* 290, 1910–1917.